HHS Public Access

Author manuscript

Nat Immunol. Author manuscript; available in PMC 2016 March 14.

Published in final edited form as:

Nat Immunol. 2015 March ; 16(3): 286–295. doi:10.1038/ni.3099.

IL-1 signaling modulates STAT activation to antagonize retinoic acid signaling and control Th17–iTreg balance

Rajatava Basu[1,5], **Sarah K. Whitley**[1,5], **Suniti Bhaumik**[1], **Carlene L. Zindl**[1], **Trenton R. Schoeb**[2], **Etty N. Benveniste**[3], **Warren S. Pear**[4], **Robin D. Hatton**[1], and **Casey T. Weaver**[1]

[1]Department of Pathology, University of Alabama at Birmingham, Birmingham, AL 35294

[2]Department of Genetics, University of Alabama at Birmingham, Birmingham, AL 35294

[3]Department of Cell, Developmental and Integrative Biology, University of Alabama at Birmingham, Birmingham, AL 35294

[4]Department of Pathology and Laboratory Medicine, University of Pennsylvania Perelman School of Medicine, Philadelphia, PA 19104 USA

Abstract

Interleukin 17 (IL-17)-producing helper (T_H17) and inducible regulatory $CD4^+$ T (iT_{reg}) cells emerge from an overlapping developmental program. In the intestines, the vitamin A metabolite retinoic acid (RA) is produced at steady state and acts as an important cofactor to induce iT_{reg} cell development while potently inhibiting T_H17 development. Here, we found that IL-1 was required to fully override RA-mediated Foxp3 expression and induce protective T_H17 responses. Through induction of an NF-κB-dependent repression of SOCS3 expression, IL-1 increased the amplitude and duration of STAT3 phosphorylation induced by T_H17-polarizing cytokines, leading to an altered balance of STAT3–STAT5 binding to shared consensus sequences in developing T cells. Thus, IL-1 signaling differentially modulated STAT activation downstream of cytokine receptors to control T_H17–iT_{reg} developmental fate.

INTRODUCTION

T_H17 and induced regulatory $CD4^+$ T (iT_{reg}) cells emerge from a shared developmental axis[1]. While transforming growth factor-β (TGF-β) contributes to developmental programming of both subsets, the pro-inflammatory cytokine interleukin 6 (IL-6) favors T_H17 development at the expense of iT_{reg} cell development[2–6]. Conversely, retinoic acid (RA), a vitamin A metabolite produced by intestinal stromal cells and dendritic cells (DCs)

Correspondence should be addressed to C.T.W. (cweaver@uab.edu).

[5]These authors contributed equally to this work.

AUTHOR CONTRIBUTIONS

R.B., S.K.W., R.D.H. and C.T.W designed the studies. R.B., S.K.W., S.B. and R.D.H. performed the experiments. C.L.Z. advised on design and execution of figures. T.R.S. performed pathological analyses. E.N.B. assisted in the design and interpretation of studies involving SOCS3. W.S.P. provided TAT-Cre peptide and provided guidance on its use in naïve $CD4^+$ T cells. R.B., S.K.W. and C.T.W. wrote and edited the manuscript.

that express retinaldehyde dehydrogenases (RALDHs)[7], acts in concert with TGF-β to promote Foxp3$^+$ expression and T_{reg} cell development while potently inhibiting T_H17 development[8–12]. A substantial percentage of T_H17 cells resident in intestinal lamina propria have expressed Foxp3 at some point during their development, indicating a dynamic relationship between Rorγt$^+$ T_H17 and Foxp3$^+$ T_{reg} cells developing in the intestines[5]. Whereas IL-6 signaling induces STAT3 phosphorylation that is required for Rorγt expression and T_H17 development, the actions of RA are at least partially dependent on IL-2, which induces STAT5 phosphorylation that is required for Foxp3 expression and iT_{reg} cell development, and which suppresses T_H17 development[9,13,14]. A number of DNA binding sites targeted by STAT3 in T_H17 lineage gene loci can also bind STAT5, providing a mechanism for competitive antagonism of these *trans*-acting factors downstream of IL-6 and IL-2 receptor signaling[15].

While IL-6 is important for reciprocally promoting T_H17 cell development and repressing iT_{reg} development, it effects in countering RA-mediated inhibition of T_H17 development are incomplete[9,14]. Thus, even at saturating doses of IL-6, T_H17 development is suppressed by RA, suggesting that additional signals might be required to override dominant RA signaling in the gut. IL-1 is another pro-inflammatory cytokine that promotes T_H17 development while subverting T_{reg} cell development[2,16], and has been shown to be important in the development of T_H17 cells in the gut, at least at steady-state[17]. However, other reports have suggested that IL-1β–IL-1R signaling is dispensable in differentiation of intestinal T_H17 cells at steady-state, based on studies of MyD88-deficient mice, which have impaired IL-1R and TLR signaling[18,19]. The role of IL-1 signaling during pathogen-induced intestinal inflammation has not been well studied. Therefore, both the mechanism of IL-1 in promoting intestinal T_H17 development as well as the role of IL-1 in T_H17 development during acute intestinal inflammation, particularly in disease models where T_H17 cells are protective, remain largely undefined[20,21].

In this study, we sought to define the role of IL-1 in regulating the developmental balance of T_H17 and T_{reg} cells, with emphasis on its effects in the intestines during challenge with the enteropathogenic bacterium, *Citrobacter rodentium*, which elicits a T_H17 pathway response that is required for host protection[3,21,22]. Our results indicate that IL-1 signaling is required to enhance IL-6 signaling to fully override RA-mediated Foxp3 expression and induce protective T_H17 responses. Through an NF-κB–dependent mechanism, IL-1 repressed the expression of suppressor of cytokine synthesis (SOCS3), a feedback inhibitor of JAK-induced tyrosine phosphorylation of STAT3. Inhibition of SOCS3 expression by IL-1 resulted in an increased amplitude and duration of STAT3 tyrosine phosphorylation downstream of signaling by T_H17-polarizing cytokines, without altering IL-2–induced STAT5 signaling tyrosine phosphorylation. IL-1 signaling therefore altered the balance of STAT3/STAT5 binding to shared consensus sequences in developing T cells, including the CNS2 element in the *Foxp3* locus that regulates stability of *Foxp3* expression, as well as target sequences in the *Il17a–Il17f* locus. Thus, IL-1 signaling differentially modulates STAT activation downstream of cytokine receptors to control T_H17–iT_{reg} cell developmental fate.

RESULTS

IL-1β reverses RA-induced inhibition of T_H17 differentiation

IL-6 counteracts the effects of RA-mediated suppression of T_H17 cell development, albeit incompletely[9]. In the course of examining the role for IL-1β in promoting T_H17 cell development, we found that, in contrast to IL-6, IL-1β completely reversed the impairment of T_H17 cell differentiation observed when DCs from mesenteric lymph nodes (MLNs) were used to activate naïve $CD4^+$ T cells (Fig. 1a,b). Moreover, IL-1β was comparable to the retinoic acid receptor (RAR) inhibitor, LE450, in blocking the effects of RA. Accordingly, addition of IL-1β overrode the inhibition of T_H17 differentiation by RA, irrespective of RA concentration (Fig. 1c,d). This result was not due to down-regulation of RAR or RXR receptor subunits, as all family members were either unchanged or modestly increased by IL-1 signaling, and occurred despite partial RA-mediated down-modulation of IL-1R1, which was highly expressed by developing T_H17 cells relative to T_H0 cells (Supplementary Fig. 1).

In extension of these studies, we examined the effects of IL-1 in reversing the expression of Foxp3 supported by RA signaling in developing T_H17 cells (Fig. 1e,f). Using T_H17 cells derived from naïve precursors of dual reporter mice (*Il17f*$^{Thy1.1}$*1Foxp3*^{gfp}), $Foxp3^+$IL-$17F^-$ cells were sorted and re-stimulated under T_H17 polarizing conditions in the absence or presence of RA addition. In the absence of added RA, a significant fraction of sorted $Foxp3^+$ cells lost Foxp3 expression and expressed IL-17F. This transition was significantly inhibited by RA, which supported retention of Foxp3 and suppressed expression of IL-17. Similar to its effects on developing T_H17 cells, IL-1 signaling overrode the effects of RA to support Foxp3 expression and IL-17 repression. Thus, IL-1 receptor signaling overrides RA-mediated induction of iT_{reg} cell programming to promote and stabilize T_H17 programming, thereby shifting the iT_{reg}–T_H17 balance in favor of T_H17 cell development.

IL-1R1 deficiency alters iT_{reg}– T_H17 balance during infection

To explore the role of IL-1 signaling in modulating the iT_{reg}–T_H17 balance *in vivo*, we examined infection by the intestinal pathogen, *C. rodentium*, protection against which is mediated by the T_H17 pathway[3,21,22]. It has been suggested from studies of steady-state intestinal T_H17 development that conflicting reports on the role of IL-1 have arisen due to use of phorbol ester (PMA) and ionomycin stimulation of recovered T cells *ex vivo*[17,23]. We therefore used wild-type and IL-1R1-deficient *Il17f*$^{Thy1.1}$*1Foxp3*^{gfp} dual reporter mice to directly examine gene expression *ex vivo* without requirement for PMA plus ionomycin or anti-CD3 stimulation-induced recall[24]. Because *Il17f* is expressed early in T_H17 development, at which time it is dominant over *Il17a* expression[24], the *Il17f*$^{Thy1.1}$ reporter model provides a sensitive read-out of early T_H17 gene expression. Moreover, the *Il17f*$^{Thy1.1}$ reporter model enables specific depletion of IL-17F–producing cells *in vivo* by administration of anti-Thy1.1 mAb[25].

Anti-Thy1.1 mAb-mediated depletion of IL-17F–producing cells in *C. rodentium*-inoculated *Il17f*$^{Thy1.1}$ reporter mice during the peak of infection (3–7 days post-infection; ref.[21], and data not shown) resulted in impaired bacterial clearance and heightened injury of the

intestinal mucosa (Fig. 2a,b and Supplementary Fig. 2a,b). Infection of mice deficient for IL-1 receptor 1 (*Il1r1*$^{-/-}$) showed similarly impaired host protection with a concomitant decrease in colonic IL-17A production but not production of interferon-γ (IFN-γ)(Fig. 2c,d). Those results are similar to our previous findings using mice deficient for IL-17 receptor A (IL-17RA) and consistent with a role for IL-1 in promoting T_H17 pathway–dependent host protection[21]. Depletion of IL-17-producing cells in *Il1r1*$^{-/-}$*Il17f*$^{Thy1.1}$ mice did not significantly alter this result, suggesting that a major effect of IL-1R1 deficiency during this period of the infection was mediated by its actions on these cells. Production of IL-22 in the infected colon was reduced in IL-1R1-deficient mice, but only at the peak time point (d7 post-infection; Supplementary Fig. 2c).

We observed a transient increase in Foxp3$^+$CD4$^+$ T cells in the large intestine and draining lymph nodes of wild-type mice during infection (days 3–5; Supplementary Fig. 3a,b), as well as a shift in the balance of IL-17$^+$ versus Foxp3$^+$ cells recovered from the large intestines of infected IL-1R1–deficient mice (Supplementary Fig. 3c,d). Therefore, we posited that infection-induced IL-1 signaling in CD4$^+$ T cells might be required to overcome T_{reg} programming that is favored in intestinal tissues by production of RA, as was observed *ex vivo*. To test this hypothesis, congenically marked CD4$^+$ T cells derived from wild-type (CD45.1$^+$) or IL-1R1–deficient (CD45.1$^-$) *Il17f*$^{Thy1.1}$ reporter mice were co-transferred into T cell receptor β-deficient (*Tcrb*$^{-/-}$) recipients, which were either untreated (uninfected) or inoculated with *C. rodentium* (infected), and the frequencies of Foxp3$^+$ and IL-17F$^+$ cells assessed (Fig. 2e,f and Supplementary Fig. 2d). Although the large majority of transferred T cells were unreactive to *C. rodentium* antigens, assessment of the frequencies of Foxp3$^+$ and IL-17F$^+$ CD4$^+$ T cells among the pool of recently activated cells in the lamina propria of the large intestine (LPL) showed a marked shift towards IL-17F expression by wild-type T cells relative to that of IL-1R1–deficient T cells (>6-fold), with a reciprocal decrease in the frequency of Foxp3$^+$ T cells (>2.5-fold). In contrast, there were no significant differences in frequencies of Foxp3$^+$ or IL-17F$^+$ cells recovered from recipient spleens. These findings are consistent with a defect in iT_{reg} to T_H17 transition of activated T cells in the absence of IL-1 signaling.

In vivo RA blockade compensates for IL-1 signaling deficiency

To further examine the possible transition of Foxp3$^+$ precursors into IL-17–producing effector cells, we tracked the fates Foxp3$^+$IL-17F$^-$ CD4$^+$ T cells isolated from infected wild-type and IL-1R1–deficient dual reporter mice (*Il17f*$^{Thy1.1}$*1Foxp3*^{gfp}) following their transfer into infected TCRβ–deficient recipients (Fig. 3a,b and Supplementary Fig. 3e). In accord with a role for IL-1 signaling to promote the silencing of Foxp3 and induction of IL-17, there was a significant increase in the frequencies of Foxp3-expressing T cells recovered from recipients of IL-1R1–deficient Foxp3$^+$ T cells compared to recipients of wild-type Foxp3$^+$ T cells, with a reciprocal deficit in IL-17–expressing T cells. We then determined whether impaired T_H17 development in IL-1R1-deficient mice was due to a failure to overcome RA-mediated repression. Infected IL-1R1-deficient mice were treated with an RAR antagonist or vehicle following inoculation with *C. rodentium* (Fig. 3c,d). Blockade of RAR signaling in infected IL-1R1-deficient mice, but not in wild-type mice, significantly reversed the deficit of IL-17–producing T cells in both the LPL and MLN, but not in spleen,

and resulted in decreased bacterial loads that were associated with protection from mucosal injury and reduced weight loss (Fig. 3e,f and Supplementary Fig. 4). Collectively, these findings identify an important role for pathogen-induced IL-1 signaling in overriding iT_{reg} cell programming favored by RA-producing intestinal DCs to induce protective T_H17 responses T cells to microbial antigens.

IL-1β counters RA-driven, IL-2–STAT5–mediated T_H17 repression

RA suppresses T_H17 cell development in favor of iT_{reg} cell development at least in part via an IL-2–dependent mechanism[9,14]. To determine whether IL-1 signaling could also modulate IL-2–dependent suppression of T_H17 differentiation, we examined the effect of addition of increasing concentrations of IL-2 to cultures of naïve $CD4^+$ T cells activated by antigen under T_H17 cell polarizing conditions, with or without the addition of IL-1β (Fig. 4a,b). In the absence of IL-1β addition, increasing concentrations of IL-2 suppressed frequencies of $IL\text{-}17^+$ cells with reciprocal increases in frequencies of $Foxp3^+$ cells as reported[14]. IL-1β abrogated the suppressive effects of IL-2, irrespective of the concentration of IL-2. Comparable effects of IL-1β on IL-17 expression and Foxp3 repression were obtained under DC-free conditions of T_H17 polarization, wherein the induction of higher concentrations of endogenously produced IL-2 favor less robust T_H17 development and higher expression of Foxp3 (Supplementary Fig. 5, and data not shown). Notably, IL-23 signaling had no comparable effect on the T_H17–iT_{reg} cell balance during the early stages of differentiation (3–4 days) when IL-1 signaling induced an enhanced T_H17 response, and addition of both IL-23 and IL-1β did not augment the effect of IL-1β alone (Supplementary Fig. 5b,c, and data not shown). So, in line with its effects to override RA-mediated repression of T_H17 differentiation, IL-1β antagonized the effects of IL-2 and this effect was independent of a requirement for IL-23 co-signaling.

The similar effects of IL-1 signaling on reversal of RA– and IL-2–mediated inhibition of T_H17 cell differentiation were consistent with our finding that production of IL-2 by T cells was enhanced ~3-fold by addition of RA at all concentrations tested (Fig. 4c). This result indicated that RA-mediated repression of T_H17 cell differentiation was due, at least in part, to enhanced IL-2 production. Consistent with the actions of IL-2 to induce heightened expression of the inducible components of the IL-2 receptor, addition of RA also up-regulated IL-2Rα (CD25) and IL-2Rβ (CD122) (Fig. 4d). Notably, neither the enhanced IL-2 production nor up-regulation of IL-2 receptor components by RA was significantly affected by IL-1β, suggesting that the principal effect of IL-1β in blocking the effects of RA was likely due to interference of IL-2 signaling downstream of receptor binding of IL-2. Accordingly, blockade of IL-2 signaling reversed the reciprocal effects of RA on the T_H17-iT_{reg} cell developmental balance similarly to that induced by IL-1β (Fig. 4e,f). Further, using $CD4^+$ T cells deficient in expression of STAT5 (and thus IL-2 signaling), the effects of RA to repress IL-17 expression in favor of Foxp3 expression were comparably impaired and were not further augmented by IL-1β signaling (Fig. 4e,f). Thus, although RA acts to enhance IL-2 production and expression of the inducible components of the IL-2 receptor by T cells, the reversal of RA-mediated effects by IL-1β signaling appears to be mediated primarily through interference of IL-2 signaling and not through altered expression of IL-2 or its receptor.

IL-1β enhances pSTAT3 via NF-κB–dependent repression of Socs3

To explore mechanisms by which IL-1 might interfere with RA-mediated modulation of IL-2 signaling, we examined the tyrosine phosphorylation of STAT5 following stimulation of T cells under T_H17 polarizing conditions, with or without addition of RA or RA plus IL-1β (Fig. 5a). Consistent with its effects to enhance expression of IL-2 and its receptor, RA enhanced tyrosine phosphorylation of STAT5 in T_H17 cells, which was not significantly altered by concurrent IL-1 signaling. In contrast, RA had no effect on IL-6–induced tyrosine phosphorylation of STAT3, whereas addition of IL-1 resulted in a substantial increase in tyrosine-phosphorylated (pY)-STAT3. The effect of IL-1 signaling resulted in both increased and more sustained STAT3 tyrosine phosphorylation (Fig. 5b), and was not limited to IL-6–induced pY-STAT3, as similar results were obtained when STAT3 was activated downstream of signaling by IL-21 (Supplementary Fig. 6) or IL-23 (Fig. 5c). Therefore, while IL-1 signaling failed to directly repress the RA-mediated enhancement of IL-2–induced pY-STAT5, it did alter the pY-STAT5/pY-STAT3 ratio through its enhancement of IL-6–, IL-21– and IL-23–induced pY-STAT3, establishing an indirect mechanism by which IL-1 acts in concert with each of the STAT3-activating T_H17 pathway cytokines to override RA-mediated, IL-2–dependent repression of T_H17 development.

Because of its failure to impact RA-mediated effects on the iT_{reg}–T_H17 balance during early differentiation (Supplementary Fig. 5), we chose IL-23, also a known pSTAT3 inducer, to further examine mechanisms by which IL-1 co-signaling might alter pSTAT3 abundance. We initially examined IL-1 effects upstream of STAT3 tyrosine phosphorylation (Fig. 5d). Addition of IL-1 significantly increased and sustained the rapid tyrosine phosphorylation of Jak2 induced by IL-23 receptor activation. Tyrosine phosphorylation of Jak2 (pYpY-Jak2) induced by IL-23 receptor heterodimerization recruits STAT3 to induce its tyrosine phosphorylation, and is competitively inhibited by the rapid expression of SOCS3 downstream of STAT3 activation[26]. We reasoned, therefore, that IL-1 might modulate Jak2 and STAT3 phosphorylation through effects on expression of SOCS3. Indeed, while IL-1 signaling alone had no effect on *Socs3* mRNA expression, it significantly inhibited the expression induced by IL-23 (Fig. 5e), indicating that IL-1–dependent inhibition of *Socs3* expression contributed to enhanced pY-STAT3.

NF-κB and MAP kinase signaling cascades are activated downstream of IL-1 receptor ligation. We therefore examined the effects of specific inhibitors of NF-κB, JNKII, Erk and p38 on IL-1–induced modulation of pY-STAT3 and *Socs3* mRNA, including a Jak2 inhibitor as a control (Fig. 5f,g and Supplementary Fig. 7). Notably, of the IL-1 signaling inhibitors examined, only NF-κB inhibitor blocked the enhancement of pY-STAT3 induced by IL-23, and was associated with reversal of the suppression of *Socs3* expression. This result suggested that IL-1–induced NF-κB activation might repress SOCS3 expression as a mechanism to enhance pY-STAT3 content. Accordingly, T_H17 cells derived from mice with deficiency of the NF-κB component, RelA, targeted to $CD4^+$ T cells (*Rela*$^{fl/fl}$*Cd4*-Cre) showed no enhancement of pY-STAT3 induction by IL-1–IL-23 co-signaling (Fig. 5h). This finding is in agreement with a study in a hepatocyte cell line[27], where, after a transient, modest early enhancement of induction, IL-1 repressed IL-6–induced SOCS3 expression via NF-κB. In addition to its effects on tyrosine phosphorylation of STAT3, we found that IL-1

signaling increased serine phosphorylation of STAT3 (pS727-STAT3) via the p38 kinase pathway (Supplementary Fig. 7a,b), an effect that has been shown to potentiate the actions of the STAT3 homodimer[28]. However, this effect was more transient and independent of a requirement of IL-23 (or IL-6) co-signaling, suggesting that any effects of STAT3 serine phosphorylation are likely to be secondary to the principal effects on tyrosine phosphorylation modulated by the NF-κB–SOCS3 axis.

Finally, an important role for IL-1–mediated repression of SOCS3 in overriding RA-mediated inhibition of T_H17 cell differentiation was directly established, as the inhibitory effect of RA was largely mitigated by specific deletion of *Socs3* in developing T_H17 cells. Thus, delivery of Cre to naïve $CD4^+$ T cells from *Socs3*$^{fl/fl}$ mice via a Tat-Cre fusion protein led to a reduction in RA-induced Foxp3 expression and enhancement of IL-17 that was comparable in presence of IL-23 or IL-1β (Fig. 6a,b). Collectively, these data identify a SOCS3-dependent mechanism by which IL-1–induced NF-κB signaling regulates the amplitude and duration of STAT3 tyrosine phosphorylation induced by T_H17-polarizing cytokines.

IL-1β modulates STAT3 vs. STAT5 binding to consensus sequences

In view of the dominant effect of IL-1 to override RA– and IL-2–induced repression of T_H17 cell development, we reasoned that the actions of IL-1 signaling to enhance STAT3 phosphorylation might overcome pSTAT5 competition for binding to shared STAT-binding consensus sequences induced by RA-dependent IL-2 signaling[15]. Chromatin immunoprecipitation (ChIP) analyses were performed to quantitate the relative binding of pSTAT3 and pSTAT5 to consensus regulatory sites in the *Il17a-Il17f* and *Foxp3* under various conditions of RA and IL-1β addition in T_H17 polarized cells activated by IL-6 alone (STAT3) or IL-6 plus IL-2 (STAT5) (Fig. 7a,b). As a control for the STAT5-dependent effects of RA, T_H17-polarized cells deficient for STAT5 (*Stat5*$^{-/-}$) were included. We found that, with the exception of the intergenic enhancer 10 kb downstream of the *Il17a* transcription start site (*Il17a*+10), all STAT3-STAT5 binding sites in the *Il17a-Il17f* locus of T_H17 cells treated with RA alone showed reciprocal, decreased STAT3 and increased STAT5 binding (Fig. 7a). The decrease in STAT3 binding caused by RA addition was reversed in STAT5-deficient cells, consistent with the actions of RA to enhance IL-2–dependent STAT5 signaling. Addition of IL-1β reversed both the RA-induced increase in binding of STAT5 and the decrease in binding of STAT3, consistent with the augmented STAT3 phosphorylation induced by IL-1 signaling (Fig. 5b–f). At the intergenic *Il17a*+10 site, both STAT3 and STAT5 binding were unaffected by addition of RA, although both were significantly affected by IL-1β, indicating that additional regulatory mechanisms might confer greater STAT3 binding at this *cis*-regulatory element, irrespective of IL-2–induced pSTAT5.

Competition between pSTAT5 and pSTAT3 binding at the CNS2 intronic enhancer of the *Foxp3* gene has been proposed to regulate the heritable maintenance of *Foxp3* expression—and thus the stability of the T_{reg} cell developmental program[29,30]. We found that RA, by enhancing STAT5 binding, also restricts IL-6-mediated STAT3-binding at CNS2 in the *Foxp3* locus during T_H17 differentiation but is outcompeted by increased STAT3 binding

promoted by IL-1. Consistent with this result, while IL-1 alone had no effect on repressing Foxp3 expression during iT_{reg} cell development (Supplementary Fig. 8a), it significantly augmented the limited extinction of Foxp3 expression induced by IL-6 in secondary cultures of sorted Foxp3$^+$ T cells derived from *Il17f*$^{Thy1.1}$*Foxp3*^{gfp} dual reporter mice (Supplementary Fig. 8b). Indeed, even in the presence of exogenous RA, which promoted Foxp3 expression stability, greater than 50% of cells extinguished their expression of Foxp3, with a significant population converting into IL-17F-producing cells. Thus, IL-1 acts cooperatively with IL-6 to subvert the Foxp3–iT_{reg} cell program in favor of T_H17 development due, at least in in part, to its actions to alter the relative binding of pSTAT3 and pSTAT5 at the key CNS2 enhancer element in the *Foxp3* locus.

DISCUSSION

The early developmental programs of iT_{reg} and T_H17 cells are intimately linked, reflected in the co-expression of lineage-specifying transcription factors Foxp3 and Rorγt downstream of TGF-β signaling[5,6]. The balance between antagonistic effects of RA and IL-2, which promote iT_{reg} cell development while suppressing T_H17 cell development, and IL-6 and IL-1, which promote T_H17 development while suppressing iT_{reg} cell development, is particularly critical in determining homeostatic versus host protective immunity to microbes in the intestines, where production of RA by resident DCs normally favors anti-microbial tolerance. Here, we show that IL-1 signaling overrides the effects of the RA–IL-2 axis in promoting iT_{reg} cell differentiation to allow a host-protective T_H17 response to an enteric pathogen, and we define a mechanism by which IL-1 signaling modulates the T_H17–iT_{reg} cell developmental balance. By enhancing the amplitude and duration of phospho-STAT3 activity induced by T_H17-specifying cytokines (for example, IL-6 and IL-23), IL-1 alters the pSTAT3/pSTAT5 ratio in developing T cells to enhance T_H17 cell development at the expense of iT_{reg} cell development. Indeed, by favoring pSTAT3 binding over pSTAT5 binding at the CNS2 intronic enhancer in the *Foxp3* locus, IL-1–dependent potentiation of STAT3 signaling directly subverts the T_{reg} cell-stabilizing function of IL-2 promoted by RA, thereby contributing to plasticity in the T_{reg} cell developmental program[14,15,31,32]. These findings extend the role of pro-inflammatory cytokines in overriding a dominant program of T_{reg} cell development in the intestines to enable the recruitment of T_H17-mediated host defense, and provide a mechanism by which IL-1 cooperates with the actions of T_H17-specifying cytokines to promote T_H17 cell development.

Although the contribution of IL-1 to T_H17 differentiation is well established[2,16], the mechanism of its action has been unclear. Here we identify a link between IL-1 signaling and repression of SOCS3 expression as a mechanism for specifically augmenting STAT3, but not STAT5, signaling. Recent studies have detailed the structural basis by which SOCS3 interacts with the gp130-Jak1 complex following ligand-mediated trans-phosphorylation of the cytoplasmic domain of IL-6–family receptors, explaining the specificity of SOCS3 for this family of receptors[33,34]—and presumably non-gp130 receptors such as the structurally related IL-23R[26]—but not the IL-2 receptor. The rapid induction of SOCS3 expression downstream of IL-6 (or IL-23) signaling provides a negative feedback loop that rapidly terminates IL-6 or IL-23 receptor signaling by inhibiting receptor-bound Jak1 or Jak2, respectively. Through repression of Socs3 expression, IL-1 indirectly sustains Jak-STAT

interactions that potentiate pSTAT3 actions. Absent comparable effects on IL-2 receptor-induced pSTAT5, IL-1 signaling effectively shifts the ratio of pSTAT3/pSTAT5 in favor of pSTAT3, providing a competitive advantage for binding of pSTAT3 to shared DNA target sequences, as demonstrated in our ChIP studies.

Interestingly, IL-1 augmented IL-21–induced pSTAT3 similarly to that induced by IL-6 and IL-23. Although the IL-21 receptor is unlike other common γ chain cytokine receptors in primarily activating STAT3, not STAT5, as far as we are aware a direct role for SOCS3 in modulating IL-21 receptor signaling has not been defined. Further studies will be needed to determine whether the IL-21 receptor is unusual among common γ chain cytokine receptors in recruiting SOCS3, or whether other effects of IL-1 signaling contribute to the increased STAT3 phosphorylation induced by IL-21. It is notable that TGF-β has been reported to contribute to T_H17 cell development through inhibition of IL-6– and IL-21–induced SOCS3 expression[35], although another study found that TGF-β also increased STAT5 phosphorylation[36], an effect not observed herein for IL-1 signaling. Thus, although both IL-1 and TGF-β might repress SOCS3 expression in concert with T_H17-polarizing cytokines, albeit via fundamentally different signaling pathways, IL-1 would appear to preferentially alter pSTAT3/pSTAT5 ratios in favor of pSTAT3. In this regard, it is of interest that T_H17 cell development can occur in the absence of TGF-β signaling—contingent on co-signaling of IL-1β with either IL-6 or IL-23 (ref. [37]). It will therefore be of interest to determine whether this effect is mediated by IL-1–induced inhibition of SOCS3.

In addition to positioning SOCS3 for inhibition of the Jak catalytic domain, docking of the SH2 domain of SOCS3 to phosphotyrosine 759 (pY^{759}) of the IL-6–activated gp130 cytoplasmic domain inhibits binding of the cytosolic tyrosine kinase, SHP2, which activates MAP and phosphatidylinositol-3-OH kinase signaling induced by IL-6, and presumably IL-23. Thus, while potentiating STAT3 phosphorylation, IL-1–mediated repression of SOCS3 might also potentiate STAT3-independent signals from the IL-6 receptor, the effects of which have not been explored. Moreover, deficiency of SOCS3 has been shown to increase STAT1 activation in myeloid cells[38], raising the possibility that IL-1–induced suppression of SOCS3 might also impact the T_H17–iT_{reg} developmental balance via modulation of STAT1. It will be of interest to examine these issues in future studies.

A previous report found that IL-1 signaling increased expression of the transcription factors IRF4 and Rorγt, both of which are required for T_H17 cell differentiation[16]. Expression of IRF4, which, unlike Rorγt[42], is central to the development of other effector cells in addition to T_H17 cells, appears to be regulated primarily by TCR signals and is STAT-independent. Hence, increased IRF expression is unlikely to be mediated by the STAT3-amplifying effects of IL-1 signaling described herein. However, through cooperative binding with the *trans*-factor BATF at consensus motifs in multiple T_H17 lineage genes[39,40], IRF4 contributes to chromatin accessibility at a number of sites that are also targeted by STAT3 (ref. [41]), as well as sites targeted by both STAT3 and STAT5 (ref. [15]). Thus, in addition to any STAT-independent effects that IL-1 signaling might have to enhance IRF4 expression, it can also indirectly modulate the effects of IRF4 actions by altering the balance of STAT binding at composite consensus sites in target genes. In contrast to IRF4, expression of Rorγt is STAT3-dependent[43]. Thus, the effects of IL-1 to augment the amplitude and

duration of STAT3 tyrosine phosphorylation likely contribute to enhanced expression of Rorγt during T_H17 cell differentiation, whether early, downstream of IL-6 signaling, or later, following expression of the IL-23 receptor.

iT_{reg} cells differ from thymic (t)T_{reg} cells in their tendency to lose Foxp3 expression during successive rounds of cell division. This reflects differences in the methylation status of CpG islands within CNS2 of the *Foxp3* locus[30,44,45]. CNS2 is highly methylated in newly generated iT_{reg} cells, whereas tT_{reg} cells and mature iT_{reg} cells have undergone demethylation of CNS2, which enables binding of Foxp3 and Runx1, among other factors, that confers stable expression of *Foxp3* under limiting IL-2 conditions[32]. Although the mechanism by which CNS2 becomes demethylated during T_{reg} cell maturation remains to be fully elucidated, it has recently been found that CNS is the major site of IL-2–induced STAT5 binding in the *Foxp3* locus[32], and, in contrast to other factors that bind CNS2, STAT5 can bind CNS2 irrespective of its methylation status[36]. Although unproven, this suggests that STAT5 might be an important factor in recruiting demethylation complexes to CNS2, in addition to its function in sustaining competency of CNS2 in immature iTreg cells as they divide[32]. Data presented herein favor a model wherein IL-1 signaling in intestinal T cells responding to enteropathogenic infection is important to override the RA–IL-2–STAT5 axis in favor of enhanced, sustained STAT3 signaling that inhibits STAT5 binding to *Foxp3* CNS2 to silence expression of Foxp3 while promoting of expression Rorγt and other T_H17 lineage genes that contain consensus sequences regulated by competitive antagonism of STAT5-STAT3 binding, thereby deviating nascent or immature iT_{reg} cells towards T_H17 cells development. These findings extend the role of pro-inflammatory cytokines in overriding a dominant program of T_{reg} cell development in the intestines to enable the recruitment of T_H17-mediated host defense, and provide a rationale for consideration of IL-1 blockade to re-establish homeostasis in the treatment of chronic inflammatory diseases mediated by the T_H17 pathway.

METHODS

Mice

The following mouse strains used were purchased from Jackson Laboratory and/or bred at our facility: C57BL/6J (B6); B6.129P2-*Tcrb*^{tm1Mom}/J (*Tcrb*$^{-/-}$); B6.129S2-*Il1b*^{tm1Dch} (*Il1b*$^{-/-}$); B6.Cg-Tg-*Il17f*$^{tm1(Thy1)Weav}$ (*Il17f*$^{thy1.1}$); B6.Cg-Tg$^{(TcraTcrb)425Cbn}$/J (OT-II); B6N.129(Cg)-*Foxp3*^{tm3Ayr}/J (*Foxp3*^{gfp}); B6.129S7-*Il1r1*^{tm1Imx}/J (*Il1r1*$^{-/-}$); B6.129S6-*Stat5a*-*Stat5b*^{tm2Mam}/Mmjax (*Stat5*$^{fl/fl}$); B6.129S1-*Rela*$^{fl/fl}$ (*Rela*$^{fl/fl}$); B6.Cg-Gt(ROSA)26Sor$^{tm14(CAG-tdTomato)Hze}$/J (*Rosa26*$^{TdTomato\ fl/+}$); and B6.129S4-*Socs3*^{tm1Ayos}/J (*Socs3*$^{fl/fl}$). B6.Cg-Tg(*Cd4*-Cre)^{1Cwi} (*Cd4*-Cre) were purchased from Taconic and B6.CD45.1 from Frederick Cancer Center. All strains were on a B6 background. All intercrosses to generate additional strains like WT and IL-1R-deficient dual reporter mice (*Il17f*$^{thy1.1}$.*Foxp3*^{gfp}), *Il17f*$^{thy1.1}$.CD45.1/CD45.2 and *Stat5b*$^{fl/fl}$. *Cd4*-Cre mice were generated by crosses in our breeding facility. Animals were bred and maintained under specific pathogen-free condition in accordance with institutional animal care and use committee regulations.

C. rodentium infection and mAb treatments

C. rodentium strain DBS100 (ATCC), was used for all inoculations with the exception of experiments where whole body imaging was performed. For imaging experiments, the bioluminescent *C. rodentium* strain ICC180 (derived from DBS100) was used[1]. This strain harbors an constitutive *luxCDABE* operon encoding luciferase of nematode *Photorhabdus luminescens. C. rodentium* strain DBS100 was grown at 37 °C in LB broth and *C. rodentium* strain ICC180 was grown in LB containing kanamycin (100 μg/ml). Mice were inoculated with 2×10^9 cfu (high dose) in a total volume of 200 ml of PBS via gastric gavage.

For depletion of *Il17f*^{thy1}.1 cells *in vivo*, mice were injected intraperitoneally (IP) with 400 μg anti-Thy1.1 (Univ. Alabama-Birmingham Epitope Recognition and Immunoreagent Core Facility, clone 19E1.2) on d3 and d7 post-infection. In all studies, age- and sex-matched mice were used (6–12 weeks of age).

Bioluminescence imaging

Mice were anesthetized with isoflurane and placed in a supine position in a custom built chamber for imaging with IVIS-100 system and Living Image Software (Xenogen, Inc.). Baseline images were collected prior to gavage with 2×10^9 cfu *C. rodentium* strain ICC180 and whole body images were taken at a binning of 4 over 1 for 3 min at the indicated times post infection with ICC180. Luminescence emitted from the same gate in individual mice was quantified as counts per second and pseudocolor images represent light intensity generated as a measure of colonization of the luminescent bacterial strain.

Cell isolation, *in vitro* T cell differentiation, protein transduction and inhibitor treatment

Naïve $CD4^+$ T cells from spleens or lymph nodes of 8–10-week-old mice were purified by flow cytometric sorting on a FACS Aria II instrument (BD Bioscience) by gating on the $CD4^+CD25^-CD62L^{hi}CD44^{lo}$ fraction. Isolated $CD4^+$ T cells were cultured in RPMI containing 10% FBS, 100 IU/ml penicillin, 100 μg/ml streptomycin, 1 mM sodium pyruvate, non-essential amino acids, 50 μM β-mercaptoethanol, and 2 mM L-glutamine (R-10). For polyclonal plate-bound stimulation, sorted $CD4^+$ T cells were stimulated with 5 μg of plate-bound anti-CD3 and 1 μg/ml of soluble anti-CD28. For polyclonal feeder-based stimulation, sorted $CD4^+$ T cells were stimulated with 1 μg/ml of soluble anti-CD3 in presence of in presence of irradiated, T-cell depleted splenic or mesenteric lymph node feeder cells obtained from *Il1b*$^{-/-}$ mice. For antigen-specific stimulation, sorted naïve OTII TCR transgenic $CD4^+$ T cells were activated with 5 μg/ml OVA peptide (OVAp) in presence of irradiated, T-cell depleted splenic feeder cells obtained from *Il1b*$^{-/-}$ mice. In all cases using feeder cells for T_H17 polarization, T cells and feeder cells were added at a ratio of 1:1. All cultures were done in a volume of 200 μl in 96-well U-bottom plates. For T_H17 or iTreg polarizations the following exogenous cytokines or antibodies were added at the indicated concentrations, unless stated otherwise: IL-6 (20 ng/ml; R&D Systems); TGF-β (2 ng/ml; R&D Systems); IL-21 (10 ng/ml; R&D Systems); IL-23 (5 ng/ml; R&D Systems); IL-1β (20 ng/ml; R&D Systems), hIL-2 (1U to 100 U; Roche), anti-IL-4 (10 μg/ml; clone XMG1.2); anti-IFN-γ (10 μg/ml; clone 11B11); anti-IL-2 (10 μg/ml; clone JES6-1A12, eBioscience). All-trans-retinoic acid (RA; Sigma) was added at various indicated concentrations (1 nM to 100 nM) and the retinoic acid antagonist LE 540 (Wako) was added at 1 μM concentration.

For purification of Foxp3^{+}CD4^{+} T cells, Foxp3-GFP^{+} cells were sorted by flow cytometry and subjected to various conditions as indicated. For purification of CD4^{+} single-positive thymocytes, CD8^{+} cells were initially removed by magnetic depletion of CD8^{+} T cells by MACS (mouse CD8α MicroBeads, Miltenyi Biotec), and CD4^{+} single-positive cells were further purified by isolation of the flow-through by MACS (mouse CD4^{+} T Cell Isolation Kit II, Miltenyi Biotec).

In experiments where cells were treated with cell signaling inhibitors, recovered cells were washed and serum-starved in complete medium for 1 h prior to addition of the following reagents, used at the indicated concentrations: Janus kinase 2 protein (JAK2) inhibitor AG490 (50 μM), JNK-Inhibitor-SP600125 (1 μM), and NF-κB inhibitor PDTC (1 μM). With the exception of PDTC (Sigma), all inhibitors were purchased from Calbiochem.

In experiments where naïve CD4^{+} T cells were transduced by TAT-Cre protein, sorted naïve CD4^{+} T cells from *Rosa26*$^{\text{TdTomato fl/+}}$reporter mice with a *lox*P-flanked STOP cassette were initially standardized by TAT-Cre transduction. Briefly cells were incubated in 1 ml of 100 μg/ml TAT-Cre peptide in serum free RPMI at 1:1 ratio for 15–20 min at 37 °C before washing and suspending into IL-7 (10 ng/ml) containing RPMI plus 10% FCS medium for 6, 12, 24 or 48 h, where maximum expression of the reporter was observed at 24 h. Subsequently sorted naïve CD4^{+} T cells from Ai14 td-Tomato reporter and *Socs3*$^{\text{fl/fl}}$ mice were treated in tandem with TAT-Cre or control peptide and cultured in IL-7-containing medium for 24 h followed by polarization under T_H17 conditions, with the additional culture modifications indicated in figure legends.

Flow cytometry and phospho-flow analysis

The following mAbs were used for flow cytometric sorting: anti CD4-eFlour 780 (eBioscience, clone RM4-5); anti-CD25-FITC (BD Pharmingen, clone 7D4); anti-CD62L-PE (eBioscience, clone MEL-14); and anti-CD44-APC (eBioscience, clone IM-7). For flow cytometric analyses and intracellular staining, the following mAbs were used: anti CD3-FITC (eBioscience, clone 145-2C11) or anti-CD3-PerCP-Cy5.5 (BD Pharmingen, clone 145-2C11); anti-CD4-PeCy7 (eBioscience, clone RM4-5); anti-IL-17A-APC (eBioscience, clone 17B7); anti-CD25-PerCP-Cy5.5 (eBioscience, clone PC61.5), anti-CD45.1 Per-Cy5.5 (eBioscience, clone A20) and anti-RORγt-PE (eBioscience, clone AFKJS-9). In brief, differentiated T_H17 cells were directly stained by anti-Thy1.1 (BD Pharmingen, clone OX-7) without secondary stimulation. Only in cases where intracellular IL-17A was detected, cells were stimulated with PMA (50 ng/ml; Sigma) and ionomycin (750 ng/ml; Calbiochem) for 4 h in the presence of Golgi Plug (BD Pharmingen). For detection of intracellular IL-17A and Foxp3 expression, cells were resuspended in Foxp3 staining Buffer (eBioscience). In all cases, LIVE/DEAD Fixable Near-IR Dead Cell Stain (Invitrogen) was included prior to surface staining to exclude dead cells in flow-cytometric analyses.

For phosphor-flow analysis, sorted naïve CD4^{+} T cells were differentiated with plate-bound anti-CD3 and soluble anti-CD28 under T_H17 polarizing conditions alone or in presence of RA or RA plus IL-1β. After 4 days, cells were briefly rested in neutral media before stimulating with IL-6 alone (50 ng/ml, R&D Systems) or with IL-2 (500 U/ml) for 20 min. The cells were then washed and suspended in pre-warmed PBS before fixing with 4%

paraformaldehyde for 10 min in a 37 °C incubator. The cells were washed again and resuspended in ice-cold phospho-wash buffer before adding chilled 100% methanol in drops and keeping incubating for 30 min followed by 2 washes in PBS containing 0.05% Tween. Before incubation in anti-pSTAT3 (anti-STAT3 PE, pY694, BD Pharmingen) or anti-pSTAT5 (anti-STAT5 AlexaFluor APC, pY694, BD Pharmingen) Ab (1 h), cells were pre-incubated in PBS-Tween containing 3% goat serum and 1 μl Fc block for 15 min. Samples were acquired on an LSRII instrument (BD Biosciences), and data were analyzed with FlowJo software (Tree Star).

Isolation and in staining of lamina propria lymphocytes

For isolation of lamina propria lymphocytes (LPLs), the large intestine was removed, cleared of luminal contents and fat, cut into small pieces and washed in chilled HBSS without Ca^{2+} or Mg^{2+}. Minced tissue pieces were incubated in presence of EDTA for 30 min and vortexed thoroughly to remove epithelial cells, then incubated in RPMI containing collagenase IV (1 mg/ml, Sigma-Aldrich), dispase (0.5 mg/ml, Gibco, Invitrogen) and DNaseI (0.25 mg/ml, Sigma-Aldrich). LP lymphocytes were collected by centrifugation. In all experiments using *Il17f*$^{thy1.1}$*Foxp3*^{gfp} reporter mice, unmanipulated LPLs were analyzed after surface staining with anti-CD3, anti-CD4, anti-CD25, anti-CD45.1, anti-TCR-β and anti-Thy1.1. For analyses using *Il1r1*$^{+/+}$*Il17f*$^{thy1.1}$ (CD45.1/CD45.2) and *Il1r1*$^{-/-}$*Il17f*$^{thy1.1}$ (CD45.2) recipient *Tcrb*$^{-/-}$ mice, unmanipulated LPLs were analyzed after surface staining with anti-TCRβ, anti-CD25, anti-CD45.1 and anti-CD90.1 and subsequently fixed in fixation buffer (Foxp3-staining buffer, eBioscience) before staining intracellularly with anti-Foxp3 mAb.

Adoptive transfers and *in vivo* LE135 treatment

For co-transfer of CD4$^+$ T cells from congenically marked *Il1r1*$^{+/+}$*Il17f*$^{thy1.1}$ (CD45.1/CD45.2) and *Il1r1*$^{-/-}$*Il17f*$^{thy1.1}$ (CD45.2) reporter mice to *Tcrb*$^{-/-}$ mice, CD4$^+$ T cells were isolated directly *ex vivo* by MACS-based depletion of PE-labeled antibodies against CD8α, CD11b, CD11c, CD19, CD45R (B220), CD49b (DX5), CD105, MHC-class II, γδ TCR and Ter-119 captured by anti-PE magnetic microbeads (Miltenyi Biotec). For co-transfers of WT and IL-1R1-deficient Foxp3$^+$ T cells, CD4$^+$Foxp3$^+$GFP$^+$IL-17F.Thy1.1$^-$ T cells were sorted by flow cytometry from *Citrobacter*-infected donor mice. In all cases, recovered T cells were transferred by IP injection at indicated doses and time-points.

For *in vivo* treatment of *Il1r1*$^{-/-}$ reporter mice with retinoic acid inhibitor LE135 (Torcis Bioscience), 100 μg of LE135 dissolved in DMSO (10 mg/ml) was gavaged in a volume of 200 μl (DMSO:PBS=1:20) from d3 through d7 PI and analyzed at d8 PI by flow cytometry or on d10 by histopathology. Control mice was gavaged on the same schedule with vehicle alone.

ELISA

For determination of cytokine concentrations *in vivo*, supernatants from differentiated T cells were collected on 3 day of culture and analyzed by capture ELISA. For determination of cytokine concentration *ex vivo*, colonic tissues from uninfected or *C. rodentium*-infected mice were collected at the indicated time points post infection, finely minced and cultured in

24-well plate for 24 h in R-10 medium supplemented with 10 μg/ml gentamicin. Supernatants were collected after centrifugation and analyzed by capture ELISA. IL-2, IFN-γ, IL-17A and IL-22 ELISAs were done using mouse quantikine ELISA kits per manufacturer's recommendations (R&D Systems).

Immunoblot

B6 $CD4^+$ T cells were cultured under T_H17 polarizing conditions for 5 d in presence of anti-CD3 and irradiated, T cell-depleted splenocytes. Following Ficoll separation to isolate viable cells, T cells were rested in neutral media and restimulated with IL-6 (20 ng/ml), IL-1β (20 ng/mL) or IL-21 (20 ng/ml) for the indicated times. Cell lysates were prepared in lysis buffer (RIPA buffer; 50 mM Tris-HCl pH?, 150 mM NaCl, 1 mM EDTA, 1% Triton X-100, 1% sodium deoxycholate, 0.1% SDS) containing a protease & phosphatase inhibitor mixture (Pierce). Protein was quantified by Bradford Assay before equivalent amounts were separated by SDS-PAGE and transferred to a PVDF membrane (Millipore). Primary antibodies were: anti-STAT3 (Cell Signaling #9132), anti-phospho-tyrosine(705)-STAT3 (Cell signaling Technology #9145), or anti-phospho-serine(727)-STAT3 (Cell signaling Technology #9134). HRP-cojugated Donkey anti-rabbit or HRP-conjuaged anti-mouse antibody (Affinity Bioreagents) were used to detect target protein by ECL detection kit (GE Healthcare or Pierce SuperSignal Dura).

Real-time PCR

Total RNA was isolated using RNeasy Isolation Kit per manufacturer's instructions (Qiagen) and treated with DNAse (Qiagen). cDNA synthesis was performed with Superscript III first-strand synthesis system (Invitrogen) and real-time PCR was performed on a Bio-Rad iCycler with primer pairs specific for cDNAs of *Il17f, Il1r1, Il1r2, IlrAcP, Rara, Rarb, Rarc, Rxra, Rxrb, Rxrc, Rorc* and 18S transcripts with iQT^M SYBR Green Supermix (Bio-rad). The primer sets were:

Il17f: for 5′-CGCCATTCAGCAAGAAATCC-3′, rev 5′-CTCCAACCTGAAGGAATTAGAACAG-3′;

Il1r1: for 5′-CCGGGCACGCCCAGGAGAA -3′, rev 5′-TCCAGCGACAGCAGAGGCAC -3′;

Il1r2: for, 5′-TCGGAGAAGCCCACAGTCCA -3′, rev, 5′-GGAGTGAGGTGCCAAGGGGC -3′;

IlrAcP: for, 5′- TTGCCACCCCAGATCTATTC -3′, rev 5′-CCAGACCTCATTGTGGGAGT -3′;

Rara: for, 5′- TCCGACGAAGCATCCAGAA -3′; rev 5′-GGTTCCGGGTCACCTTGTT -3′;

Rarβ: for, 5′- CAGTGAGCTGGCCACCAAGT -3′; rev, 5′-GCGATGGTCAGACCTGTGAA -3′;

Rarγ: for, 5′- GTCAGCTCCTGTGAAGGCTGC -3′; rev, 5′-GTTTCGATCGTTCCTTACAG -3′;

Rxrα: for, 5′- TAGTCGCAGACATGGACACC -3′; rev, 5′- GTTGGAGAGTTGAGGGACGA -3′;

Rxrβ: for, 5′- GCACAGAAACTCAGCCCATT -3′; rev, 5′- CATCCTCATGTCACGCATTT -3′;

Rxrγ: for, 5′- GCCTGGGATTGGAAATATGA -3′; rev, 5′- ACACCGTAGTGCTTCCCTGA -3′;

Rorc: for, 5′-CAGCCAACATGTGGAAAAGCT-3′; rev, 5′- GGGAAGGCGGCTTGGA-3′

Cd25: for, 5′- TACAAGAACGGCACCATCCTAA -3′; rev, 5′- TTGCTGCTCCAGGAGTTTCC -3′

Cd122: for, 5′- GTCCATGCCAAGTCGAACCT-3′; rev, 5′- GGATGCCTGCCTCACAAGAG -3′ Socs3 for, 5′- AGTGCAGAGTAGTGACTAAACATTACAAGA-3′; rev, 5′- AGCAGGCGAGTGTAGAGTCAGAGT-3′

18SrRNA: for: 5′- GCCGCTAGAGGTGAAATTCTTG -3′; rev, 5′- CATTCTTGGCAAATGCTTTCG -3′.

Reactions were run in duplicate and samples were normalized to 18S as a fold-induction over controls unless otherwise stated.

Chromatin immunoprecipitation (ChIP) assay

$CD4^+$ single-positive thymocytes from WT or *Stat5*$^{fl/fl}$.*Cd4*-Cre mice were polarized for 3-4 d under T_H0 (no cytokine) or T_H17 polarizing conditions (IL-6 + TGF-β), with or without RA or RA + IL-1β, followed by 20 min stimulation in CO_2 incubator by addition of IL-6 (50 ng/ml, R&D Systems) or IL-2 (500 U/ml). The cells were cross-linked with 1% (vol/vol) formaldehyde for 5 min, quenched with 125 mM glycine and then suspended in HALT protease-inhibitor containing PBS. Chromatin Immunoprecipitation (ChIP) was performed with ExactaChIP Kit from R&D systems in accordance with the manufacturer's instruction. Briefly, cells were suspended in lysis buffer containing protease-inhibitor and immunoprecipitated overnight (4 °C) with biotinylated anti-STAT3 (R&D systems) or anti-STAT5 (R&D systems). Bound DNA was collected using agarose-streptavidin beads and purified with QIAprep Spin Miniprep Kit (Qiagen). Immunoprecipitated DNA was quantitated by real-time PCR with iQTM SYBR Green Supermix (Bio-rad) on a Bio-Rad iCycler using following primer pairs specific for the indicated elements in the *Il17a-Il17f* locus[2] and *Foxp3* locus.

Il17a-5: for, 5′- CAGGTATTATTCTCAGGGCTTTGG -3′; rev 5′- TGGCAATGGTGTCTTTTCTTTG -3′

Il17aP: for, 5′- CACCTCACACGAGGCACAAG -3′; rev 5′- ATGTTTGCGCGTCCTGATC -3′

Il17a+10: for, 5′- GGATTAAGGGCACACGTGTTG -3′; rev 5′- TTTCCCCACTCTGTCTTTCCA -3′

Il17a+28: for, 5′- TCATCGGCTCCCACACAGA -3′; rev 5′- GGCAGTACCGAAGCTGTTTCA -3′

Il17fP: for, 5′- CCCACAAAGCAACACTCTTGTC -3′; rev 5′- ACTGCATGACCCGAAAGCA -3′

Il17f-5: for, 5′- GCATCGCATCTTTCAAACCA -3′; rev 5′- TTAGGATAAGCGCCCAGTGAAT -3′

Foxp3 CNS2 for, 5′-GTTGCCGATGAAGCCCAAT-3′; rev 5′- ATCTGGGCCCTGTTGTCACA-3′

Data are expressed as relative values normalized to the input DNA samples (percentage of input).

Histolopathological evaluation

Tissue samples obtained from proximal, middle and distal portions of large intestines were fixed in 10% neutral buffered formalin, embedded in paraffin to prepare 5 μm sections and stained with H&E. The tissue sections were examined and scored to evaluate tissue pathology, as previously described[3]. In all scoring, the identity of specimens was concealed from the pathologist.

Statistical analysis

For statistical analyses, *P*-values were calculated by paired or unpaired Student's *t*-test, unless stated otherwise in figure legends. $P < 0.05$ was considered significant.

Supplementary Material

Refer to Web version on PubMed Central for supplementary material.

Acknowledgments

We thank H. Qin (University of Alabama at Birmingham), L. Xu (University of Pennsylvania) and members of the Weaver laboratory for their helpful advice and comments. We are grateful to G. Frankel and S. Wiles (Imperial College, London) for provision of the bioluminescent *C. rodentium* strain and T. DeSilva (University of Alabama at Birmingham) for provision of *Rosa26*$^{TdTomato\ fl/+}$ mice. We also thank B.J. Parsons for expert technical assistance, G. Gaskins for editorial assistance, and the UAB Small Animal Imaging Facility, UAB Center for AIDS Research Flow Cytometry Core, and UAB Epitope Recognition and Immunoreagent Core Facility for imaging studies, flow cytometric sorting, and antibody preparations, respectively. This work was supported by grants from the NIH (PO1DK71176 and R01DK093015 to C.T.W. and R.D.H., and R01AI047833 to W.S.P.) and the Crohn's and Colitis Foundation of America (C.T.W, R.B. and D.B.O.).

References

1. Basu R, Hatton RD, Weaver CT. The T_H17 family: flexibility follows function. Immunol Rev. 2013; 252:89–103. [PubMed: 23405897]
2. Veldhoen M, Hocking RJ, Atkins CJ, Locksley RM, Stockinger B. TGFβ in the context of an inflammatory cytokine milieu supports de novo differentiation of IL-17-producing T cells. Immunity. 2006; 24:179–189. [PubMed: 16473830]
3. Mangan PR, et al. Transforming growth factor-β induces development of the T_H17 lineage. Nature. 2006; 441:231–234. [PubMed: 16648837]

4. Bettelli E, et al. Reciprocal developmental pathways for the generation of pathogenic effector T_H17 and regulatory T cells. Nature. 2006; 441:235–238. [PubMed: 16648838]
5. Zhou L, et al. TGF-beta-induced Foxp3 inhibits T_H17 cell differentiation by antagonizing RORγt function. Nature. 2008; 453:236–240. [PubMed: 18368049]
6. Littman DR, Rudensky AY. T_H17 and regulatory T cells in mediating and restraining inflammation. Cell. 2010; 140:845–858. [PubMed: 20303875]
7. Vicente-Suarez I, et al. Unique lamina propria stromal cells imprint the functional phenotype of mucosal dendritic cells. Mucosal Immunol. 2014; 8:141–151. [PubMed: 24938743]
8. Chen W, et al. Conversion of peripheral $CD4^+CD25^-$ naive T cells to $CD4^+CD25^+$ regulatory T cells by TGF-β induction of transcription factor Foxp3. J Exp Med. 2003; 198:1875–1886. [PubMed: 14676299]
9. Mucida D, et al. Reciprocal T_H17 and regulatory T cell differentiation mediated by retinoic acid. Science. 2007; 317:256–260. [PubMed: 17569825]
10. Coombes JL, et al. A functionally specialized population of mucosal CD103+ DCs induces Foxp3+ regulatory T cells via a TGF-beta and retinoic acid-dependent mechanism. J Exp Med. 2007; 204:1757–1764. [PubMed: 17620361]
11. Benson MJ, Pino-Lagos K, Rosemblatt M, Noelle RJ. All-trans retinoic acid mediates enhanced T reg cell growth, differentiation, and gut homing in the face of high levels of co-stimulation. J Exp Med. 2007; 204:1765–1774. [PubMed: 17620363]
12. Sun CM, et al. Small intestine lamina propria dendritic cells promote de novo generation of Foxp3 T reg cells via retinoic acid. J Exp Med. 2007; 204:1775–1785. [PubMed: 17620362]
13. Davidson TS, DiPaolo RJ, Andersson J, Shevach EM. IL-2 is essential for TGF-β-mediated induction of $Foxp3^+$ T regulatory cells. J Immunol. 2007; 178:4022–4026. [PubMed: 17371955]
14. Laurence A, et al. Interleukin-2 signaling via STAT5 constrains T helper 17 cell generation. Immunity. 2007; 26:371–381. [PubMed: 17363300]
15. Yang XP, et al. Opposing regulation of the locus encoding IL-17 through direct, reciprocal actions of STAT3 and STAT5. Nat Immunol. 2011; 12:247–254. [PubMed: 21278738]
16. Chung Y, et al. Critical regulation of early Th17 cell differentiation by interleukin-1 signaling. Immunity. 2009; 30:576–587. [PubMed: 19362022]
17. Shaw MH, Kamada N, Kim YG, Nunez G. Microbiota-induced IL-1beta, but not IL-6, is critical for the development of steady-state T_H17 cells in the intestine. J Exp Med. 2012; 209:251–258. [PubMed: 22291094]
18. Atarashi K, et al. ATP drives lamina propria T_H17 cell differentiation. Nature. 2008; 455:808–812. [PubMed: 18716618]
19. Ivanov II, et al. Induction of intestinal Th17 cells by segmented filamentous bacteria. Cell. 2009; 139:485–498. [PubMed: 19836068]
20. Ishigame H, et al. Differential roles of interleukin-17A and -17F in host defense against mucoepithelial bacterial infection and allergic responses. Immunity. 2009; 30:108–119. [PubMed: 19144317]
21. Basu R, et al. Th22 cells are an important source of IL-22 for host protection against enteropathogenic bacteria. Immunity. 2012; 37:1061–1075. [PubMed: 23200827]
22. Zheng Y, et al. Interleukin-22 mediates early host defense against attaching and effacing bacterial pathogens. Nat Med. 2008; 14:282–289. [PubMed: 18264109]
23. Hirota K, et al. Fate mapping of IL-17-producing T cells in inflammatory responses. Nat Immunol. 2011; 12:255–263. [PubMed: 21278737]
24. Lee YK, et al. Late developmental plasticity in the T helper 17 lineage. Immunity. 2009; 30:92–107. [PubMed: 19119024]
25. Harrington LE, Janowski KM, Oliver JR, Zajac AJ, Weaver CT. Memory CD4 T cells emerge from effector T-cell progenitors. Nature. 2008; 452:356–360. [PubMed: 18322463]
26. Chen Z, et al. Selective regulatory function of Socs3 in the formation of IL-17-secreting T cells. Proc Natl Acad Sci USA. 2006; 103:8137–8142. [PubMed: 16698929]

27. Yang XP, et al. Dual function of interleukin-1beta for the regulation of interleukin-6-induced suppressor of cytokine signaling 3 expression. J Biol Chem. 2004; 279:45279–45289. [PubMed: 15308667]
28. Wen Z, Zhong Z, Darnell JE Jr. Maximal activation of transcription by Stat1 and Stat3 requires both tyrosine and serine phosphorylation. Cell. 1995; 82:241–250. [PubMed: 7543024]
29. Laurence A, et al. STAT3 transcription factor promotes instability of nTreg cells and limits generation of iTreg cells during acute murine graft-versus-host disease. Immunity. 2012; 37:209–222. [PubMed: 22921119]
30. Zheng Y, et al. Role of conserved non-coding DNA elements in the Foxp3 gene in regulatory T-cell fate. Nature. 2010; 463:808–812. [PubMed: 20072126]
31. Murphy KM, Stockinger B. Effector T cell plasticity: flexibility in the face of changing circumstances. Nat Immunol. 2010; 11:674–680. [PubMed: 20644573]
32. Feng Y, et al. Control of the inheritance of regulatory T cell Identity by a cis element in the *Foxp3* locus. Cell. 2014; 158:749–763. [PubMed: 25126783]
33. Babon JJ, Varghese LN, Nicola NA. Inhibition of IL-6 family cytokines by SOCS3. Semin Immunol. 2014; 26:13–19. [PubMed: 24418198]
34. Kershaw NJ, et al. SOCS3 binds specific receptor-JAK complexes to control cytokine signaling by direct kinase inhibition. Nat Struct Mol Biol. 2013; 20:469–476. [PubMed: 23454976]
35. Qin H, et al. TGF-beta promotes Th17 cell development through inhibition of SOCS3. J Immunol. 2009; 183:97–105. [PubMed: 19535626]
36. Ogawa C, et al. TGF-β-mediated Foxp3 gene expression is cooperatively regulated by Stat5, Creb, and AP-1 through CNS2. J Immunol. 2014; 192:475–483. [PubMed: 24298014]
37. Ghoreschi K, et al. Generation of pathogenic T(H)17 cells in the absence of TGF-beta signalling. Nature. 2010; 467:967–971. [PubMed: 20962846]
38. Lang R, et al. SOCS3 regulates the plasticity of gp130 signaling. Nat Immunol. 2003; 4:546–550. [PubMed: 12754506]
39. Glasmacher E, et al. A genomic regulatory element that directs assembly and function of immune-specific AP-1-IRF complexes. Science. 2012; 338:975–980. [PubMed: 22983707]
40. Li P, et al. BATF-JUN is critical for IRF4-mediated transcription in T cells. Nature. 2012; 490:543–546. [PubMed: 22992523]
41. Ciofani M, et al. A validated regulatory network for Th17 cell specification. Cell. 2012; 151:289–303. [PubMed: 23021777]
42. Ivanov II, et al. The orphan nuclear receptor RORγt directs the differentiation program of proinflammatory IL-17^{+} T helper cells. Cell. 2006; 126:1121–1133. [PubMed: 16990136]
43. Yang XO, et al. STAT3 regulates cytokine-mediated generation of inflammatory helper T cells. J Biol Chem. 2007; 282:9358–9363. [PubMed: 17277312]
44. Miyao T, et al. Plasticity of Foxp3^{+} T cells reflects promiscuous Foxp3 expression in conventional T cells but not reprogramming of regulatory T cells. Immunity. 2012; 36:262–275. [PubMed: 22326580]
45. Ohkura N, et al. T cell receptor stimulation-induced epigenetic changes and Foxp3 expression are independent and complementary events required for Treg cell development. Immunity. 2012; 37:785–799. [PubMed: 23123060]
46. Wiles S, Pickard KM, Peng K, MacDonald TT, Frankel G. In vivo bioluminescence imaging of the murine pathogen *Citrobacter rodentium*. Infect Immun. 2006; 74:5391–5396. [PubMed: 16926434]
47. Yang XP, et al. Opposing regulation of the locus encoding IL-17 through direct, reciprocal actions of STAT3 and STAT5. Nat Immunol. 2011; 12:247–254. [PubMed: 21278738]
48. Bleich A, et al. Refined histopathologic scoring system improves power to detect colitis QTL in mice. Mamm Genome. 2004; 15:865–871. [PubMed: 15672590]

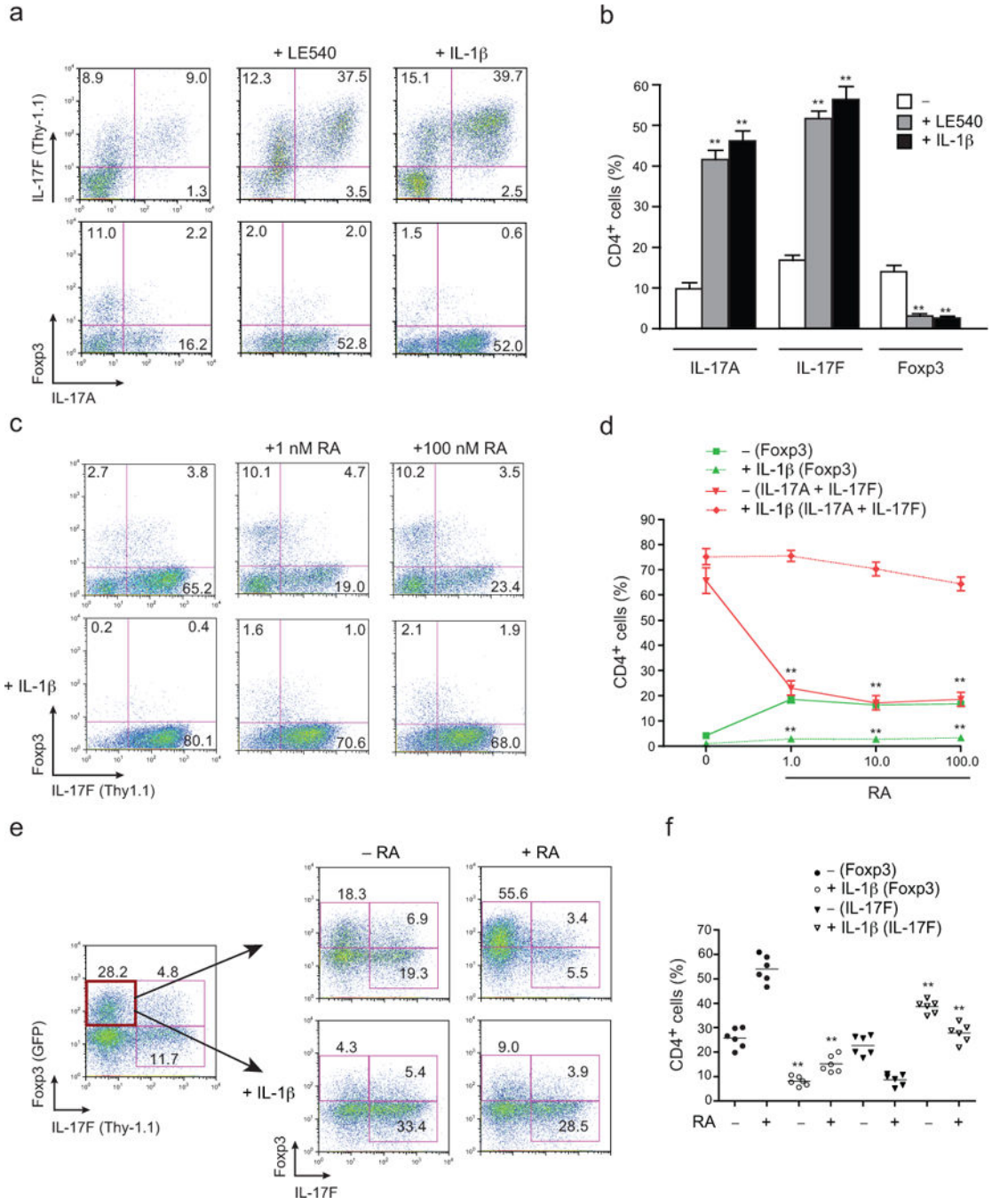

FIGURE 1. IL-1β counteracts RA-dependent inhibition of T_H17 cell development

(**a**) Naïve CD4$^+$ T cells (CD4$^+$CD25$^-$CD62L^{hi} CD44^{lo}) from *Il17f*$^{thy1.1}$ mice were activated with soluble anti-CD3 on DCs isolated from mesenteric lymph nodes (MLNs) of IL-1β–deficient (*Il1b*$^{-/-}$) mice under T_H17 polarizing conditions, with the indicated additions of an at-RA inhibitor (LE540; 1 μM) or IL-1β (20 ng/ml). Cells recovered on day 4 were stained for surface CD4 and Thy1.1 (IL-17F), and intracellular IL-17A and Foxp3, and analyzed by flow cytometry. Numbers are percentages of cells in each quadrant. (**b**) Pooled data from **a** showing frequencies of IL-17A, IL-17F (Thy1.1) and Foxp3 single producers among CD4$^+$

T cells. (**c**) Expression of Thy1.1 (IL-17F) and Foxp3 from naïve $CD4^+$ T cells from *Il17f*$^{thy1.1}$ mice activated with soluble anti-CD3 and *Il1b*$^{-/-}$ DCs under T_H17 polarizing conditions with or without IL-1β, in presence or absence of indicated concentration of at-RA at day 4. (**d**) Pooled data from **c** showing total frequencies of IL-17A–, IL-17F (Thy1.1)– and Foxp3–expressing $CD4^+$ T cells. (**e**) Naïve $CD4^+$ T cells from *Il17f*$^{thy1.1}$.*Foxp3*^{gfp} mice were activated with plate-bound anti-CD3 and soluble anti-CD28 under T_H17 polarizing conditions. On day 4 of primary culture the Thy1.1$^-$GFP$^+$ fraction of cells were sorted by flow cytometry and further cultured under T_H17 conditions with or without IL-1β (20 ng/ml), in the presence or absence of at-RA (1 nM). On day 4 of secondary culture, frequencies of IL-17F (Thy1.1) versus Foxp3-GFP$^+$ cells were determined after surface staining of Thy1.1 (IL-17F) and flow cytometry. Numbers are percentages of cells in the each quadrant. (**f**) Pooled data from secondary cultures from **e** showing frequencies of Foxp3$^+$ (GFP) and IL-17F$^+$ (Thy1.1) $CD4^+$ T cells. Data are representative of one of three similar independent experiments (**a**); pooled from three independent experiments with nine samples (n = 9) per group (**b**); representative of one of three similar independent experiments (**c**); pooled from three experiments with twelve samples (n = 12) per group (**d**); representative of one of two independent experiments (**e**); or pooled from two independent experiments with six samples (n = 6) per group (**f**). Data are means and s.e.m. in **b**,**d**,**f**. $^{**}P < 0.01$ (two-tailed unpaired t-test).

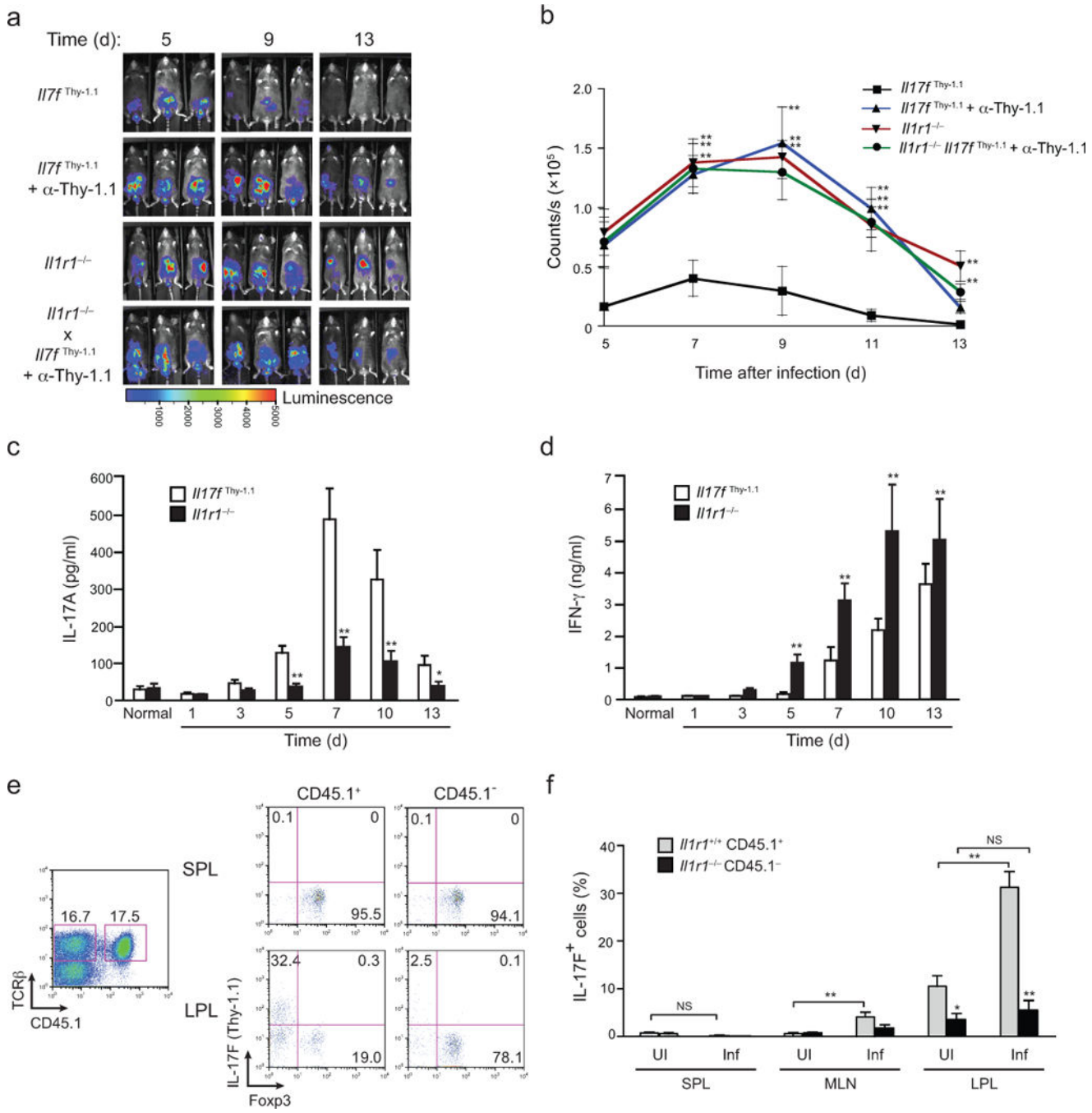

FIGURE 2. IL-1R signaling is required for host-protective T_H17 and T_{reg}–T_H17 cell balance *in vivo*

(**a**) Serial whole-body imaging of untreated *Il17f*$^{thy1.1}$ mice, *Il17f*$^{thy1.1}$ mice treated with depleting anti-Thy1.1 mAb or *Il1r1*$^{-/-}$ mice or *Il1r1*$^{-/-}$ mice treated with depleting anti-Thy1.1 mAb after inoculation with luminescent strain of *C. rodentium* and imaged at the indicated days post infection. (**b**) Colonization kinetic data from **a** represented as counts/sec at different time points post-infection with *C. rodentium*. (**c**,**d**) Quantitative ELISA of IL-17A (**c**) and IFNγ (**d**) in supernatants from cultured homogenates of colonic tissue

collected from *Il17f*$^{thy1.1}$ and *Il1r1*$^{-/-}$ mice at the indicated times after inoculation with *C. rodentium*. (**e**) 3 × 10^6 of donor *Il1r1*$^{+/+}$.*Il17f*$^{thy1.1}$ (CD45.1/CD45.2) and *Il1r1*$^{-/-}$.*Il17f*$^{thy1.1}$ (CD45.2) CD4$^+$ T cells were mixed and co-transferred to recipient *Tcrb*$^{-/-}$ mice that were either uninfected or infected with *C. rodentium* 2 weeks post-reconstitution (see Supplementary Fig. 2d for schematic). Seven days later, expression of Thy1.1 (IL-17F) and intracellular Foxp3 by CD45.1$^+$ and CD45.1$^-$ splenic lymphocyte (SPL) and colonic lamina propria lymphocytes (LPL) from reconstituted recipient *Tcrb*$^{-/-}$ mice was analyzed (gated on activated CD4$^+$ T cells). Numbers in each quadrant indicate the frequency of cells. Single plot represents equal frequencies of *Il1r1*$^{+/+}$ and *Il1r1*$^{-/-}$ TCRβ$^+$ cells within reconstituted mice. (**f**) Frequencies of IL-17F (Thy1.1) cells in *Il1r1*$^{+/+}$ CD45.1$^+$ and *Il1r1*$^{-/-}$ CD45.1$^-$ populations of SPL, MLN and LPL of uninfected and infected recipient *Tcrb*$^{-/-}$ mice. Data are: representative of one of two similar independent (*Il1r1*$^{-/-}$ mice treated with depleting anti-Thy1.1 mAb) or one of three similar independent experiments (*Il17f*$^{thy1.1}$ mice, *Il17f*$^{thy1.1}$ mice treated with depleting anti-Thy1.1 mAb or *Il1r1*$^{-/-}$ mice) **a;** pooled from two or three independent experiments with nine to eleven mice per group **b;** from two independent experiments with six mice per group **c**,**d;** representative of one of two similar independent experiments **e;** or pooled from two independent experiments with six mice per group **f.** Data are means and s.e.m. in **b**,**c**,**d**,**f**. N.S.= Not significant, **P* < 0.05 and ***P* < 0.01 (two-tailed unpaired *t*-test).

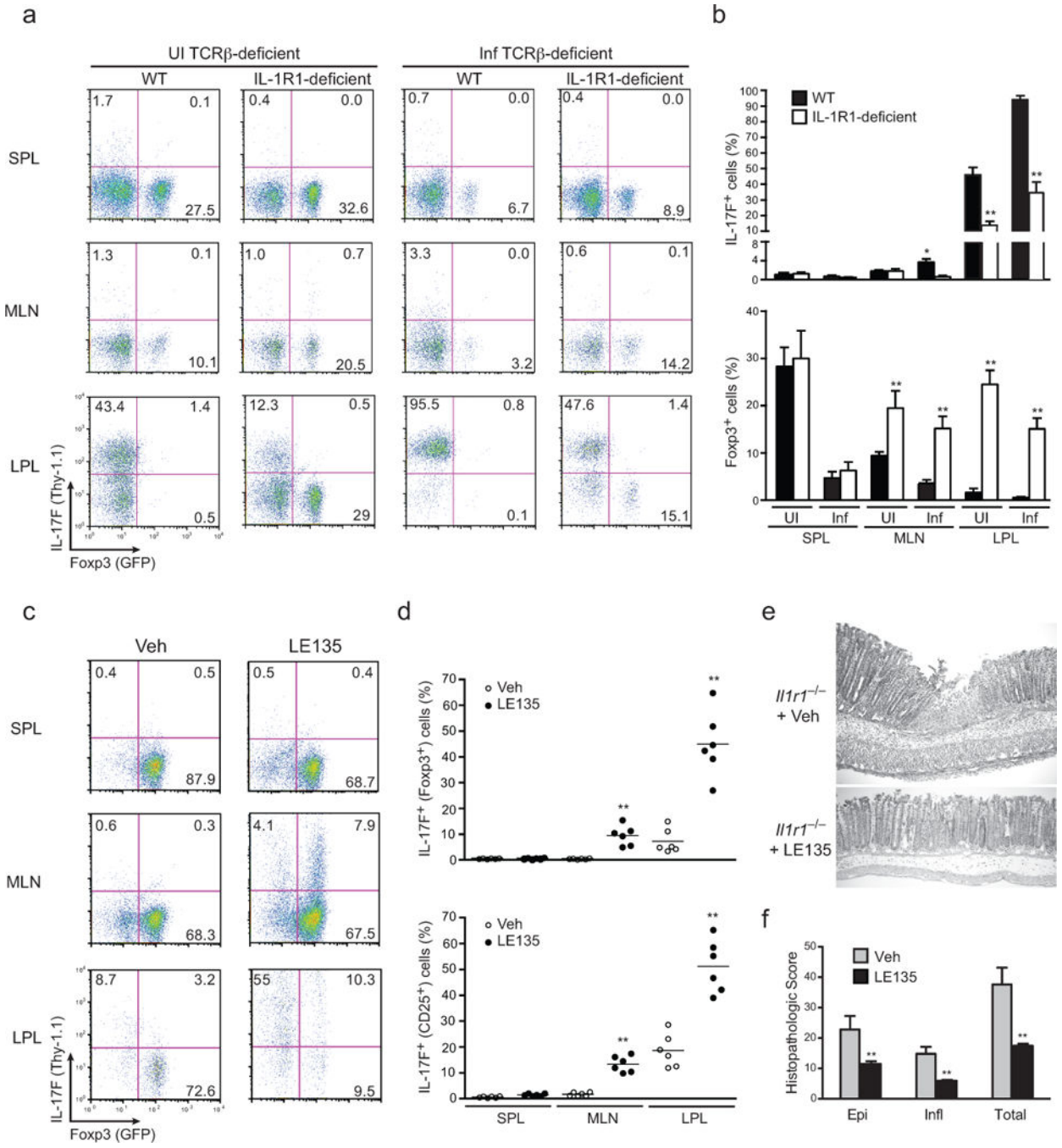

FIGURE 3. In absence of IL-1β, *in vivo* blockade of RA facilitates iT_{reg} to T_H17 cell conversion during enteropathogenic bacterial infection

(a) 2.5×10^6 $Foxp3^+IL\text{-}17F^-$ $CD4^+$ T cells of infected donor *Il1r1*$^{+/+}$.*Il17f*$^{thy1.1}$.*Foxp3*^{gfp} and *Il1r1*$^{-/-}$.*Il17f*$^{thy1.1}$.*Foxp3*^{gfp} mice were collected and sorted on day 2 post-infection (PI) and transferred to recipient TCRβ–deficient (*Tcrb*$^{-/-}$) mice that were either uninfected or infected with *C. rodentium* 2 days before (see Supplemental Fig. 3e for schematic). Expression of Thy1.1 (IL-17F) and Foxp3-GFP on splenic, MLN and LP isolates of uninfected recipient *Tcrb*$^{-/-}$ or d2 infected recipient *Tcrb*$^{-/-}$ was analyzed 8 days post-

infection. Splenic, MLN and LP lymphocytes were isolated and analyzed without restimulation *ex vivo* for Thy1.1 (IL-17F) and Foxp3-GFP expression by flow cytometry after gating on TCRβ$^+$ cells. Numbers indicate the frequencies in each quadrant. (**b**) Frequencies of splenic, MLN and colonic IL-17F (Thy1.1) cells and Foxp3-GFP cells as prepared in **b**. (**c**) Expression of Thy1.1 (IL-17F) and Foxp3 (GFP$^+$) CD4$^+$CD25$^+$ T cells in *Il1r1*$^{-/-}$.*Il17f*$^{thy1.1}$.*Foxp3*^{gfp} mice that were inoculated with 2 × 10^9 cfu *C. rodentium* and gavaged with vehicle alone or with retinoic acid inhibitor (LE135) on days 3–7 post infection. On d8 PI, mice were sacrificed and frequencies of Thy1.1 (IL-17F) and Foxp3 (GFP$^+$) CD4$^+$CD25$^+$ T cells in spleen, MLN and lamina propria were assessed by flow cytometry without restimulation *ex vivo*. (**d**) Frequencies of Thy1.1 (IL-17F) and Foxp3 (GFP$^+$) expression within Foxp3$^+$ (GFP$^+$) and activated (CD4$^+$CD25$^+$) fractions from splenic, MLN and lamina propria lymphocytes of vehicle treated or LE135 treated *C. rodentium* infected *Il1r1*$^{-/-}$.*Il17f*$^{thy1.1}$.*Foxp3*^{gfp} mice. (**e**) Representative histopathology of H&E-stained colonic tissues sections derived from vehicle–treated or LE135–treated, *C. rodentium*–infected *Il1r1*$^{-/-}$.*Il17f*$^{thy1.1}$.*Foxp3*^{gfp} mice at d10 PI. (**f**) Histopathology scoring of colons from untreated or LE135 treated, infected *Il1r1*$^{-/-}$.*Il17f*$^{thy1.1}$.*Foxp3*^{gfp} mice processed on d10 PI. Data are: representative of one of three similar independent experiments **a;** pooled from three independent experiments with 10 mice per group **b;** representative of one of two similar independent experiments **c;** pooled from two independent experiment with 6 mice per group where each point indicates one mouse **d;** representative of one of two independent experiments **e**; or pooled from two independent experiments with 4 mice per group **f.** Data are means and s.e.m. in **b**,**d**,**f**. *P < 0.05 and **P < 0.01 (two-tailed unpaired *t*-test

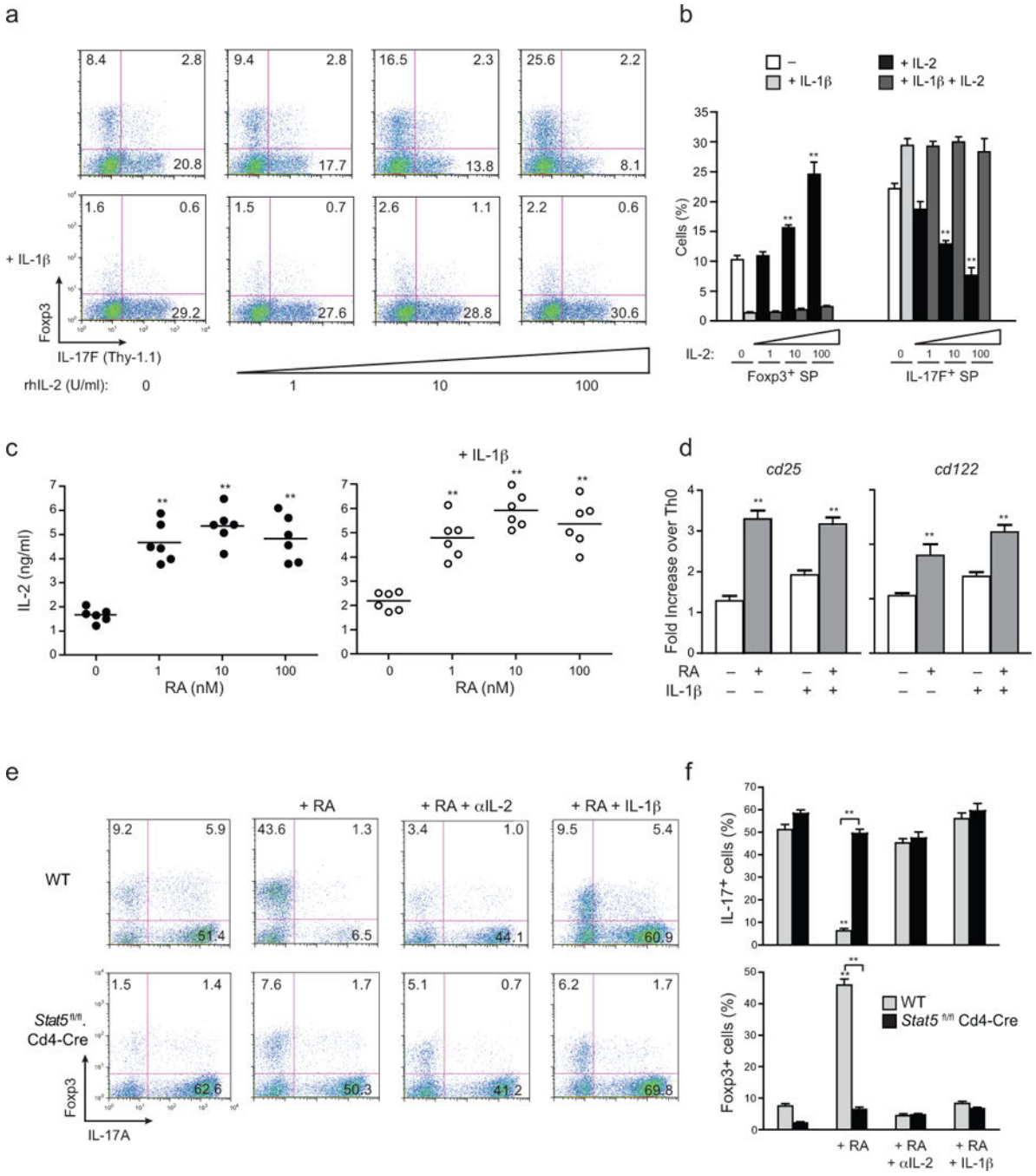

FIGURE 4. IL-1β counteracts RA-driven IL-2/STAT5–dependent repression of T_H17 development

(**a**) Expression of Thy1.1 (IL-17F) and Foxp3 from naïve OTII-Tg CD4 T cells ($CD4^+CD25^-CD62L^{hi}CD44^{lo}$) from OTII.*Il17f*$^{thy1.1}$ mice activated with OVA peptide and IL-1β–deficient DCs for 4 days under T_H17 polarizing conditions, with or without IL-1β addition, and with or without addition of the indicated doses of rhIL-2 at day 4. (**b**) Frequencies of Foxp3 and IL-17F single-producers from OTII-Tg $CD4^+$ T cells polarized as in **a** at indicated concentrations of rhIL-2 (**c**) Quantitative IL-2 ELISA from supernatants of

naïve $CD4^+$ T cells from *Il17f*$^{thy1.1}$ mice that were activated with plate-bound anti-CD3 and soluble anti-CD28 under T_H17 polarizing conditions in absence (left) or presence (right) of IL-1β addition, with or without addition of addition of RA at the indicated concentrations (1–100 nM). (**d**) Expression of *Cd25* and *Cd122* transcripts by quantitative RT-PCR from naïve $CD4^+$ T cells from *Il17f*$^{thy1.1}$ mice that were activated with plate-bound anti-CD3 and soluble anti-CD28 under T_H17 polarizing conditions in absence or presence of IL-1β, with or without addition of RA (1 nM) at 60 h. Expression values are normalized to T_H0 controls. (**e**) Expression of IL-17A and Foxp3 from MACS-purified $CD8^-CD4^+$ thymocytes isolated from WT B6 or *Stat5*$^{fl/fl}$.*Cd4*-Cre mice that were activated with soluble anti-CD3 and *Il1b*$^{-/-}$ splenic DCs under T_H17 polarizing condition (IL-6+TGF-β with or without the indicated additions of RA (1 nM), anti-IL-2 (10 μg/ml) and IL-1β (20 ng/ml) for 4 days. (**f**) Frequencies of IL-$17A^+$ and $Foxp3^+$ from $CD4^+$ T cells from WT B6 or *Stat5*$^{fl/fl}$.*Cd4*-Cre mice as treated in (**e**). Data are: representative of one of three similar independent experiments **a**; pooled from three independent experiments with nine samples per group (n = 9) **b**; pooled from two independent experiments with six samples (n = 6) **c**; representative of two independent experiments with 6 samples per group (n = 6) where individual data points represent each sample **d**; representative of one of three similar independent experiments **e**; or pooled from three independent experiments with ten samples (n = 10) per group **f.** Data are means and s.e.m. in **b**,**c**,**d**,**f**). $^{**}P < 0.01$ (two-tailed unpaired T-test).

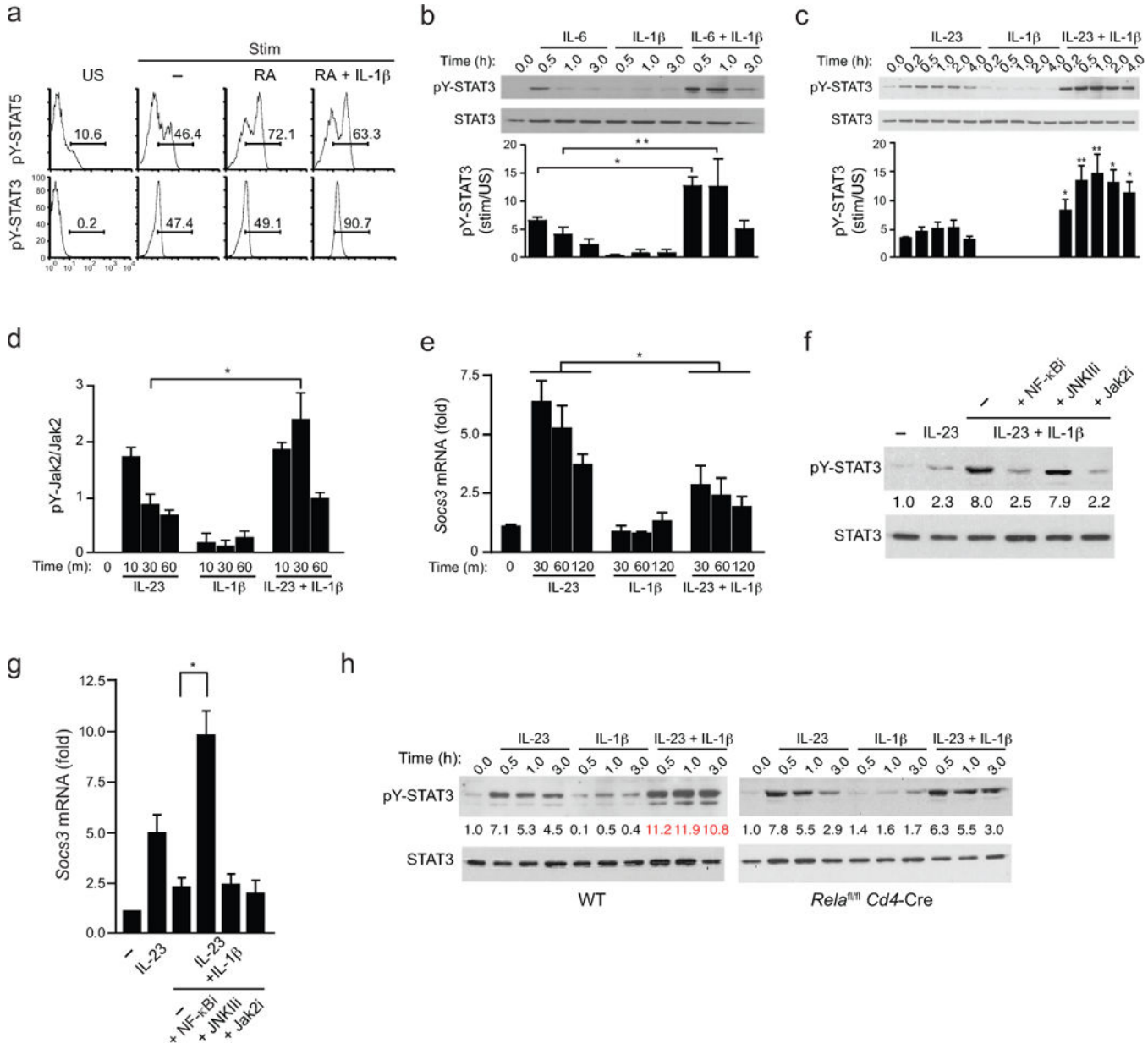

FIGURE 5. NF-κB-dependent SOCS3 repression by IL-1β enhances amplitude and duration of STAT3 phosphorylation

(**a**) Intracellular pSTAT5 and pSTAT3 analysis from naïve CD4$^+$ T cells from WT B6 mice that were activated with plate-bound anti-CD3 and soluble anti-CD28 under T_H17 polarizing conditions (IL-6 +TGF-β with or without the indicated additions of RA and IL-1β for 4 days. Prior to analysis, IL-6 and IL-2 were added to cultures for 20 min and intracellular pSTAT5 and pSTAT3 were determined by flow cytometry. (**b**) Expression of phospho-tyrosine(705)-STAT3 (pY-STAT3) from naïve CD4$^+$ T cells cultured under T_H17 polarizing conditions for 4–5 days, then restimulated with IL-6 alone, IL-1β alone, or both for indicated time periods. Cell lysates were harvested, immunoblotted with antibody directed against phospho-tyrosine(705)-STAT3 (pY-STAT3) or total STAT3 (top). (**c**) Expression of phospho-tyrosine(705)-STAT3 (pY-STAT3) by immunoblot from naïve CD4$^+$ T cells that

were cultured under T_H17 polarizing conditions for 4 days, then restimulated with IL-23 alone, IL-1β alone, or both for indicated time periods and assessed as in **b**. (**d**) Quantitative analysis of active phosphorylated form of Jak2 from naïve $CD4^+$ T cells that were cultured for under T_H17-polarizing conditions and activated as in **c**, then lysed and subjected to ELISA analysis that quantified both the active phosphorylated form of Jak2 [Jak2(pYpY1007/1008)] and total Jak2. pYpY-Jak2 values were normalized to total Jak2 expression and data are expressed as fold change over unstimulated T_H17 cells where unstimulated cells were assigned a value of 1. (**e**) Expression of *Socs3* transcripts by quantitative RT-PCR from naïve $CD4^+$ T cells that were cultured under T_H17 conditions as in **c** and restimulated with IL-23 and/or IL-1β for the indicated times. Transcript abundance of *Socs3* were normalized against β2-microglobulin and relative expression compared to unstimulated cells was calculated using the ΔΔCt method. (**f**) Expression of phospho-tyrosine(705)-STAT3 (pY-STAT3) by immunoblot from naïve $CD4^+$ T cells polarized under T_H17 conditions were isolated and pre-treated with indicated signaling inhibitors for 1 h then either left unstimulated or treated with IL-23 +/− IL-1β before cell lysates were harvested and immunoblotted for pY-STAT3 and total STAT3 as in **c**. Average values of pooled data representing relative expression of IDVs of pY-STAT3 normalized to total STAT3 are shown (between upper and lower panels). (**g**) Expression of *Socs3* transcripts by quantitative RT-PCR from naïve $CD4^+$ T cells polarized under T_H17 conditions were isolated, pre-treated with the indicated signaling inhibitors for 1 h, were then restimulated with IL-23 and/or IL-1β for 45 min and harvested for RNA isolation and *Socs3* mRNA quantification as in **e**. (**h**) Expression of phospho-tyrosine(705)-STAT3 (pY-STAT3) by immunoblot from naïve $CD4^+$ T cells from WT and $Rela^{fl/fl}$.*Cd4*-Cre mice were polarized and analyzed as in **c**. Average values of pooled data representing relative expression of IDV of pY-STAT3 normalized to total STAT3 are shown (between upper and lower panels). Data are: representative of one of two similar experiments **a;** representative of one of three similar independent experiments (**b**,**c**); pooled from two independent experiments with six samples ($n = 6$) per group **d;** three independent experiments with nine samples ($n = 9$) per group **e;** pooled from two independent experiments with nine samples ($n = 9$) per group **g;** representative of one of two similar independent experiments (**f**,**h)** where numbers in red (IL-23 + IL-1β) are significantly different ($P < 0.01$) from corresponding values for cells stimulated with IL-23 alone (mean and s.e.m. in **b**,**c**,**d**,**e**,**g)**. * $P < 0.05$ and ** $P < 0.01$ (two-tailed unpaired *t*-test).

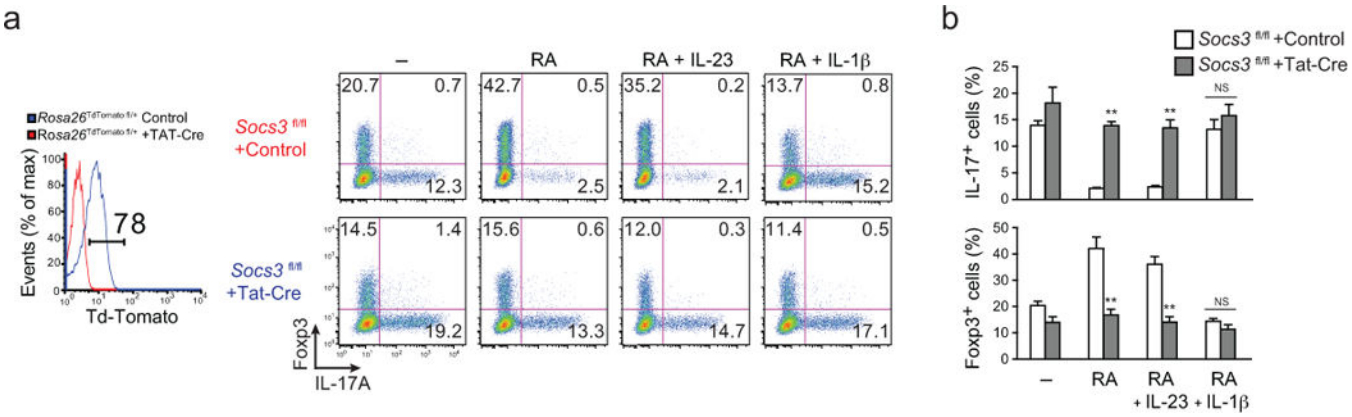

FIGURE 6. Deletion of SOCS3 abrogates the IL-1–dependent reversal of RA repression of T_H17 development

(**a**) Expression of Foxp3 and IL-17A (right composite panel) in naïve $CD4^+$ T cells from *Socs3*$^{fl/fl}$ mice (control, red; Tat-Cre, blue) that were cultured under T_H17 polarizing conditions with the indicated additions of RA, IL-1β and IL-23 with or without Tat-Cre peptide and Td-Tomato protein expression (left single plot) from *Rosa26*-floxed-STOP-TdTomato reporter mice (*Rosa26*$^{TdTomato\ fl/+}$) treated with or without Tat-Cre peptide and cultured similarly under T_H17 conditions and analyzed for Cre-mediated deletion efficiency. Numbers indicate the frequencies in each quadrant. (**b**) Frequencies of IL-17A– and Foxp3–positive cells from $CD4^+$ T cells treated as in (**a**). Data are representative of one of four (deletion efficiency analysis with *Rosa26*$^{TdTomato\ fl/+}$) or one of two (*Socs3*$^{fl/fl}$ with or without Tat-Cre) independent experiments (**a**) or are pooled from two independent experiments with 12 samples (n = 12) per group (**b**). Data are means and s.e.m. in **b**. NS = not significant, ** $P < 0.01$ (two-tailed unpaired t-test).

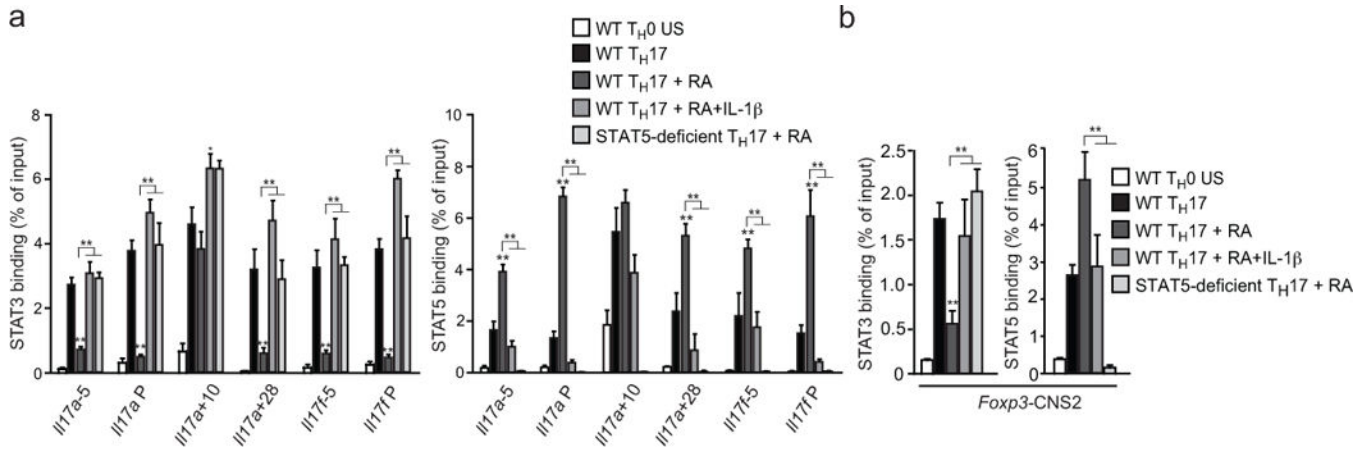

FIGURE 7. IL-1β reverses RA-mediated STAT5 binding in the *Il17a-Il17f* and *Foxp3* gene loci

(**a,b**) Chromatin immunoprecipitation (ChIP) analysis of STAT3 and STAT5 binding in purified $CD4^+CD8^-$ thymocytes isolated from wild-type (WT) or *Stat5*$^{fl/fl}$.*Cd4*-cre mice and activated with plate-bound anti-CD3 and soluble anti-CD28 under T_H0 or T_H17 conditions (IL-6 +TGF-β, with or without the indicated additions of RA and IL-1β. On day 4, recovered cells were stimulated with IL-6 (pSTAT3) or IL-6+IL-2 (pSTAT5) and processed for ChIP-PCR to quantitate binding of STAT3 or STAT5 to the indicated sites within the *Il17a-f* (**a**) and *Foxp3* (**d**) gene loci. Unstimulated T_H0 cells were used as a negative control. Results are relative to input DNA. Data are representative of two independent experiments with 3 replicates per experiment (means and s.e.m. in **a**, **b**). **P* < 0.05 and ***P* < 0.01 (two-tailed unpaired *t*-test).